Environmental Earth Sciences (2021) 80:608
https://doi.org/10.1007/s12665-021-09884-0

ORIGINAL ARTICLE

# Sea-level rise impact and future scenarios of inundation risk along the coastal plains in Campania (Italy)

Gianluigi Di Paola[1] · Angela Rizzo[2] · Guido Benassai[3] · Giuseppe Corrado[4] · Fabio Matano[5] · Pietro P. C. Aucelli[6]

Received: 24 September 2020 / Accepted: 30 July 2021
© The Author(s) 2021

## Abstract

Sea-level rise as a consequence of global warming increases the need to analyze coastal risks to conceive adaptation strategies aimed at coping with marine impacts at both short- and long-term scales. In this context, this study presents future scenarios of inundation risk evaluated along the main alluvial coastal plains of the Campania region (Italy). Due to their geomorphological and stratigraphical setting, the investigated areas are characterized by low topography and relevant but variable subsidence rates. Based on the upgrade of already published data and the new analysis of available datasets derived by multi-temporal interferometric processing of satellite Synthetic Aperture Radar (SAR) images, future scenarios of local sea level for the years 2065 and 2100 have been evaluated coupling global projections with local subsidence trends. Furthermore, aspects related with the distribution of natural and anthropic assets, as well as the local social vulnerability, have been taken into account to calculate the overall risk. The inundation risk maps here proposed can effectively address the request to improve the knowledge of policymakers and local administrators and to raise their awareness about the potential impacts of climate change in coastal areas.

**Keywords** Relative sea-level rise · Multi-Temporal SAR Interferometry · Coastal subsidence · Climate change

## Introduction

As demonstrated in many of the most recent works regarding the analysis of climate data on a global and regional scale (Chen et al. 2017; Dieng et al. 2017; Yi et al. 2017; Copernicus Climate Change Service 2018, 2020; Nerem et al. 2018; Dangendorf, et al. 2019, World Meteorological Organization 2019), one of the most evident consequences of global warming is the acceleration in Global Sea Level Rise (GSLR). Future projections provided by the Intergovernmental Panel on Climate Change (IPCC) for the end of the twenty-first century show a global sea level increasing up to 1 m above the reference period (1986–2005) (IPCC, 2014, and related updated data in IPCC 2019). The expected changes in sea level will potentially lead to the permanent submersion of coastal low-lying areas with negative impacts on natural ecosystems and anthropic settings (Nichols 2010). This phenomenon is locally enhanced by Vertical Ground Deformation Movements (VGDMs), which characterize wide coastal areas worldwide. In fact, several areas around the world present natural subsidence trends that have been accelerated since the last century by human causes, such as the increased exploitation of the natural resources (oil and fluid extraction, mining) and the groundwater over-pumping (Brambati et al. 2003; Teatini et al. 2012; Schaeffer et al. 2012; Pappone et al. 2012; IPCC, 2014; Shirzaei and Bürgmann 2018a, b; Wright et al. 2019). In Italy, almost all the alluvial coastal plains, both on the Tyrrhenian and Adriatic coasts, are characterized by subsidence that locally causes severe modifications in Relative Sea Level (RSL) trends

✉ Angela Rizzo
angela.rizzo@uniba.it

1 Department of Biological, Geological, and Environmental Sciences (BiGeA), University of Bologna "Alma Mater Studiorum", Bologna, Italy

2 Department of Earth and Geo-environmental Sciences, University of Bari "Aldo Moro", Bari, Italy

3 Department of Engineering, University of Naples "Parthenope", Naples, Italy

4 Dipartimento delle Culture Europee e del Mediterraneo, Basilicata University, Matera, Italy

5 Istituto di Scienze Marine (ISMAR), Consiglio Nazionale delle Ricerche (CNR), Naples, Italy

6 Department of Science and Technology, University of Naples "Parthenope", Naples, Italy

Published online: 26 August 2021

(Antonioli and Silenzi 2007; Baldi et al. 2009; Lambeck et al. 2011; Cenni et al. 2013; Aucelli et al. 2017a; Ruberti et al. 2017; Matano et al. 2018; Amato et al. 2020).

In this context, the main international guidelines for the assessment and management of the coastal flooding events were first provided in the framework of the Flood Directive (EC 2007), which forces the Member States to provide inundation maps also accounting for the expected climate change impacts, and then better defined in the EU Adaptation Strategy on Climate Change (European Commission 2013), which was adopted in 2013 by the European Commission with the aim of making Europe more climate-resilient and enhancing the preparedness and capacity of communities to respond to the expected impacts of climate change. In particular, the EU Adaptation Strategy stresses that coastal zones are particularly vulnerable to the impact of sea-level rise, challenging the climate resilience and adaptive capacity of coastal societies. In addition, it is widely recognized that the application of coastal adaptation measures for protecting communities from coastal floods will also have a very high economic benefit. This last aspect has been deeply addressed in a recent study published by Vousdoukas et al. (2020), where a comprehensive analysis of economically efficient protection scenarios along Europe's coastlines was performed. According to this study, Italy has more than 50% of coasts where benefits of adaptation exceed the costs. Furthermore, in case that no coastal adaptation and risk-reduction measures will be implemented, accelerated sea-level rise in view of global warming could result in unpreceded coastal losses along Europe's coastlines (Vousdoukas et al. (2018). To support and assist policy-makers and co-ordinators on the national level in identifying, implementing, monitoring and evaluating climate change adaptation strategies, the European Commission issued the "*Guidelines on developing adaptation strategies*" where the key features of the adaptation policy process are provided. Based on these guideline, the Adaptation Support Tool has been developed as a practical guidance tool by the EC in collaboration with the EEA. This tool provides the steps to be followed for the definition of a national adaptation strategy. In particular, Step 2 "Assessing climate change risks and vulnerabilities" identifies the comprehensive analysis of current and future climate risks as a basis for the definition of adaptation strategies and plans.

In accordance with the most recent international requirements for climate adaptation and risk reduction, our study aims to evaluate the impact of future RSL along the main coastal plains of the Campania Region (southern Italy), which are considered to be particularly prone to sea impacts due to the presence of wide areas characterized by very low topography, reaching a total surface of approximately 30 $km^2$ (Aucelli et al. 2017a, b; Di Paola et al. 2018). Nowadays, these areas are mostly affected by retreat processes mainly due to both human activities, related to the exploitation of the littoral zone and watershed, and natural causes, related to the increasing intensity of marine coastal processes, such as erosion and flooding, associated to the sea-level increase occurred during the last decades in the Tyrrhenian area (Spano et al. 2020). The investigated coastal plains are characterized by wide inhabited areas (such as the coastal sectors of the municipalities of Castel Volturno, Mondragone, Salerno, Castellamare di Stabia) and present a high socio-economic value due to the presence of several touristic infrastructures, wide protected wetland areas, and a number of coastal archaeological sites (such as Paestum and Velia) that can be considered vulnerable to the potential effects of processes linked to marine agents (Mattei et al. 2019, 2020). Coastal processes related to the sea-level rise are therefore expected to cause negative impacts on the local and regional socio-economic settings, as already documented for the Volturno River coastal plain, where recent marine storms coupled with extreme river discharges (dated January 2014, February 2015, October 2015, November 2018; December 2019) have caused floods in the main streets, damages to the beach touristic activities, and displacements of a number of householders, especially along the right side of the Volturno River (Moccia 2018; Frasca 2018; La Repubblica 2019).

According to the most recent definitions, the risk of climate-related impact results from the interaction of the climate-related hazards with the exposure and the vulnerability of human and natural systems (IPCC 2014). The hazard analysis is, therefore, a preliminary step for to the evaluation of future coastal risk scenarios, which require the identification of the natural and anthropic assets located in the hazard prone zone and, for this reason, potentially exposed to be impacted by sea.

Based on the upgrade of already published data (Aucelli et al. 2017a, 2018; Di Paola et al. 2018) and new analysis of available datasets derived by multi-temporal interferometric processing of satellite Synthetic Aperture Radar (SAR) images, this study evaluates future local sea levels and related inundation risk scenarios for the years 2065 and 2100 along the coastal plains in Campania (Italy). The analyses here proposed allow obtaining: (i) maps of future coastal inundation hazard, intended as the proneness of the investigated plains to be impacted by sea inundation; (ii) maps of coastal exposure and vulnerability; (iii) maps of future coastal inundation risk.

## Study area

Campanian coastal plains are the result of the complex interaction among sedimentary inputs, tectonics and eustatism (Patacca et al. 1990; Casciello et al. 2006; Sacchi et al. 2014). The coastal plains along the western flank of the Apennine chain originated during the Pliocene and

Early Pleistocene as half-graben structures in extensional tectonic regime induced by the opening of the Tyrrhenian Sea (Patacca et al. 1990). Their sedimentary history has been influenced by a general subsiding tendency that favored the deposition, during the Quaternary, of very thick (thousand meters) sedimentary successions. Depending on the intensity of subsidence rates, sedimentation rates and eustatic sea-level oscillations, these plains were repeatedly invaded and abandoned by the sea (Ippolito et al. 1973; Brancaccio et al. 1991, 1995; Cinque et al. 1995; Cinque 1991).

Volturno, Sele, Sarno and Alento rivers have originated the largest coastal plains in Campania Region (Fig. 1). They are characterized by flat topography and are mostly formed by clayey, silty and sandy marine, alluvial and marsh deposits, including about 500 km long sandy beaches.

Geomorphological evolution of these coastal plains has been deeply investigated in past studies (Cinque 1991; Cinque et al. 1995; De Pippo et al. 2000; Alberico et al. 2012a; 2012b; Pappone et al. 2011, 2012; Amorosi et al. 2012; Pennetta et al. 2016; Ruberti & Vigliotti 2017; Ruberti et al. 2017; Donadio et al. 2018; Ascione et al. 2020; Amato et al. 2020; Corrado et al. 2020). Their physiography and sedimentary architecture have been influenced in a somewhat different way by the coastal response to Holocene sea-level rise induced by the climatic warming that followed the last glacial maximum (LGM) (Brancaccio et al. 1995).

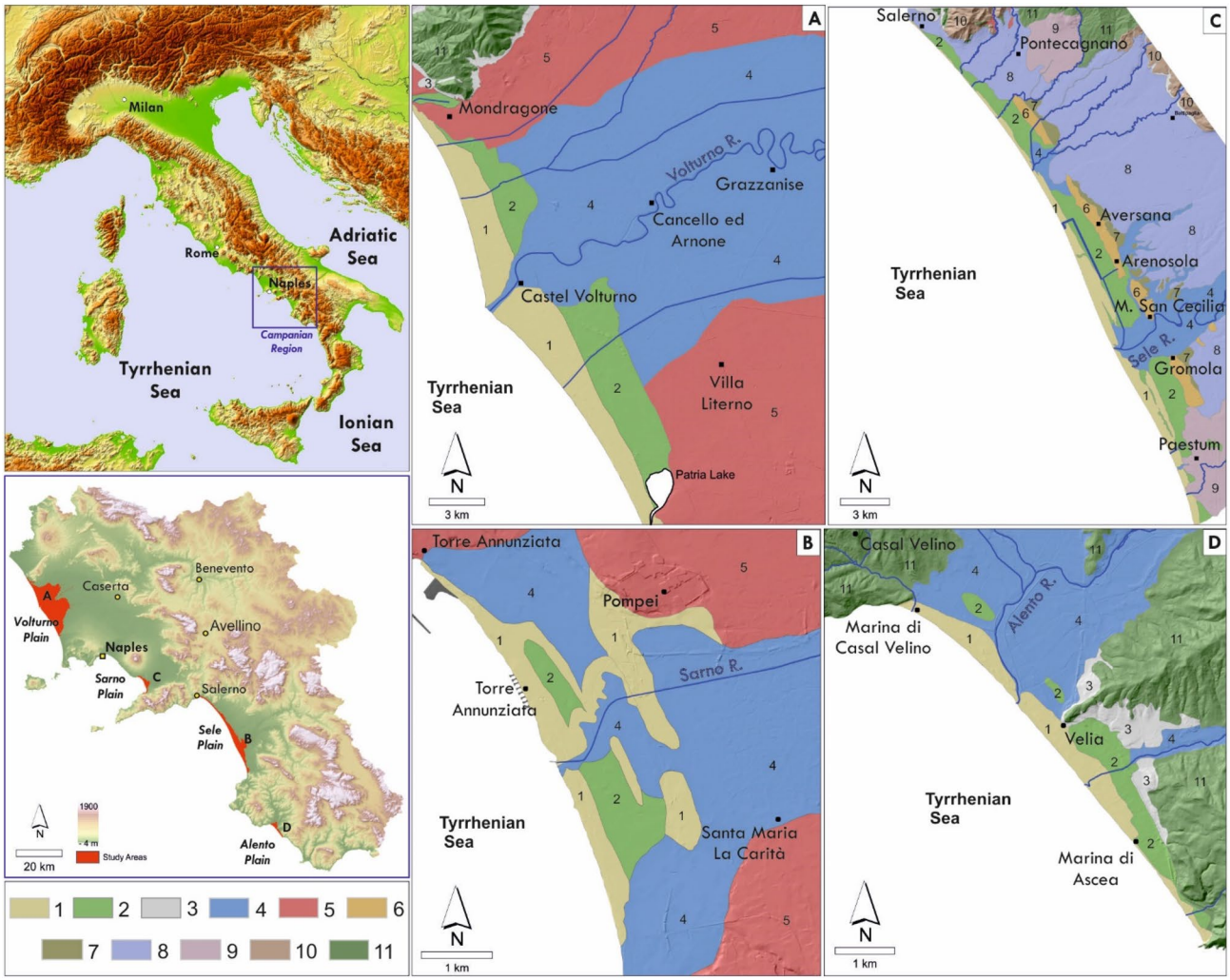


**Fig. 1** Study area. Investigated coastal areas with simplified geological maps of Volturno (**a**), Sarno (**b**), Sele (**c**) and Alento (**d**) plains. Legend: (1) Dunal ridge deposits (Holocene); (2) Lagoon and marsh deposits (Holocene); (3) Slope waste deposits (Late Pleistocene–Holocene); (4) Fluvial deposits (Late Pleistocene–Holocene); (5) Volcaniclastic deposits (Quaternary); (6) Dunal ridge deposits (Late Pleistocene); (7) Lagoon and marsh deposits (Late Pleistocene); (8) Marine, continental and transitional deposits (Middle–Late Pleistocene); (9) Travertine deposits (Middle Pleistocene–Holocene); (10) Eboli Conglomerates Formation (Early Pleistocene); 11) Pre-Quaternary bedrock

The Volturno coastal plain (Fig. 1) was largely submerged by the sea since mid-late Pleistocene thanks to tectonic subsidence related to extensional faults bordering the plain. This plain was aggraded greatly after the highly explosive eruption of Campanian Ignimbrite (CI) (40 ky BP; Giaccio et al. 2017) whose deposits covered the entire Campania plain when the sea level was about 50 m below today (Aiello et al. 2021). These volcanoclastic deposits represent the substrate for the uppermost Pleistocene–Holocene sedimentation (Romano et al. 1994; Corrado et al. 2018; Mastrocicco et al. 2019). After the LGM the postglacial sea-level rise caused a rapid flooding of the lower sector of the Volturno valley (Romano et al. 1994; Amorosi et al. 2012; Ruberti et al. 2018b). Since approximately 6.5 ky BP, a coastal progradation phase established, allowing the onset of the present-day alluvial plain characterized by a flat morphology. The plain is bordered seaward by a 35 km long sandy beach-dune system, behind which there is a wide lowland area with elevation comprised between – 2 m and 0 m a.s.l. This area is a remnant of a retrodunal depression, which is characterized by clayey and silty deposits, locally interbedded with peat layers (Amorosi et al. 2012). From the analysis of the present-day topography, it emerges that the extent of the area currently below sea level is equal to 26.2 $km^2$ (corresponding to 14.5% of the investigated area).

The Sarno coastal plain (Fig. 1) experienced subsidence of at least 30 m over the last 130,000 years (Barra et al. 1989; Cinque 1991; Cinque & Irollo 2004; Valente et al. 2019; Santo et al. 2019), as indicated by the beach deposits of the Euthyrrenian transgression that are present in the subsoil of the plain at altitudes never higher than -25 m a.s.l. The late stages of coastal progradation that followed the maximum Holocene ingression reached ~ 8 km inland of the present-day coastline (Cinque 1991). Based on age constraints on the sediments buried at shallow depths, the Holocene subsidence postdates the maximum Holocene ingression in the southwestern part of the Sarno Plain (e.g., Albore Livadie et al. 1990; Aucelli et al. 2017b). The current morphology of the Sarno Plain is partly due to the continuation of subsidence until historical times and partly to the lack of significant solid load within the Sarno River waters coming from large karst springs located on the edge of the plain (Cinque et al. 1991). From the analysis of the present-day topography, it emerges that the extent of area currently below sea level is equal to 0.12 $km^2$ (corresponding to 1.4% of the investigated area).

The Sele coastal plain (Fig. 1) is characterized by an elongated beach-dune ridge formed by Gromola-S. Cecilia and Arenosola–Aversana paleoridges originated during the Last Interglacial period (MIS 5, Brancaccio et al. 1987, 1988; Russo and Belluomini 1992). Based on chrono-altimetric data of the MIS 5 palaeo-sea level, the plain experienced a slight uplifting during the last 100–120 ky (Brancaccio et al. 1988; Barra et al. 1998, 1999). The back-barrier domains were filled up with marshy and fluvio-palustrine sediments when the sea-level rise stopped and aeolian sands finally accumulated on the coastal ridges. Remnants of the back-barrier terrace related to these high-stand phases are preserved in the modern landscape at 11–14 m a.s.l., while the coeval shore-face sediments occur up to 13 m a.s.l. and the dunes up to 23 m a.s.l. The present coastline testifies the evolution of the Holocene barrier-lagoon system (Amato et al. 2012). A composite sandy ridge forms a dune system with a mean height of about 3 m a.s.l. currently interrupted by rivers and artificial drainage channels. The large back-ridge depression, having a mean height of about 0.5–1.5 m a.s.l., hosted palustrine and marshy environments (Alberico et al. 2012b), that have been artificially drained and are, today, prone to marine inundation. From the analysis of the present-day topography, it emerges that the extent of area currently below sea level is equal to 1.30 $km^2$ (corresponding to 2.2% of the investigated area).

The infill of the plain is not homogeneous (Amato et al. 2020) because of the presence of unconsolidated deposits with different degrees of compaction. Dunal and coastal sands, back-ridge (lagoonal and palustrine) silty clays, and thick peaty layers are the main facies of this sedimentary sequence (Amato et al. 2020). Such features could promote local subsidence, mainly in sectors where the silty clays and peaty layers show higher thickness, as in the back-barrier sectors of the plain (Amato et al. 2020).

The Alento coastal plain (Fig. 1) is considerably aggraded by Late Quaternary fluvial and transitional deposits. An initial filling dates back to the Last Interglacial period and is partly covered by alluvial fans during the Last Glacial period. The peaking stage of the Holocene ingression transformed the lower Alento valley into a ria, penetrating about 2.5 km inland of the present shoreline (Cinque et al. 1995). During the last millennia, this ria has been gradually filled, and the coastline moved forward thanks to high rates of fluvial supply (Cinque et al. 1995). Nowadays, the coastal plain is characterized by different orders of dune cords at different distances from the current coastline. These dunes consist mainly of clay and silty-clay deposits and have maximum heights between 3.5 m and 5.5 m, and are interspersed in depressed areas with no more than 0.5 m of altitude differences. From the analysis of the present-day topography, it emerges that the extent of the area currently below sea level is equal to 0.03 $km^2$ (corresponding to 0.4% of the investigated area).

Observational data from tide gages and marine buoys allow providing a general characterization of the study area in terms of sea-level oscillations and wave conditions. In particular, data recorded in three tide gage stations sector that can be considered representative of the investigated Tyrrhenian coastal sector (Napoli 40°50′54″N, 14°16′1″E,

Salerno 40°40′35″N, 14°16′18″E and Palinuro 40°1′47″N, 15°16′31″E), downloaded from the Permanent Service for Mean Sea Level (PSMSL) website (https://www.psmsl.org/), show increasing rates of 4.5 mm/yr (Salerno), 7.6 mm/yr (Napoli) and 9.1 mm/yr (Palinuro) for the period 2001–2015. Local tide gage series are referred to a period shorter than the recommended 30-year long period suggested by the World Meteorological Organization (WMO 2017) and, for this reason, the estimated rates can be biased. Nevertheless, they are representative of a general increasing trend that is confirmed also by the analysis of the continuous series collected by the Italian Institute of Environmental Protection and Research (ISPRA 2015) for the most recent period (2015–2020). For the characterization of the wave conditions, it is possible to refer to the data acquired recorded by the Ponza buoy (40°52′00″N, 12°57′00″E, 115 m depth), which is included in the Italian Sea Wave Measurement Network and it can be considered representative of the offshore wave conditions of the study area. In this case, data analysis (referred to the period 1989–2010) shows that the study area is frequently affected by moderate wave conditions coming mainly from SSW to NNW sector. A maximum value of Hs (6.90 m) was recorded in December 1999 while the medium annual maximum value is 4.31 m. Furthermore, in a recent study (Buonocore et al. 2020), the results of the analysis carried out by considering an 18-year-long (2002–2019) tide-gage dataset collected on the Island of Ischia (Southern Tyrrhenian Sea; Gulf of Naples) were presented. In this case, the results indicate that RSL rise in Ischia has a magnitude of 3.9 mm/year. Regarding the astronomical tide, the study area experiences a typical semi-diurnal tide with a maximum value of 0.30 m.

The investigated Campanian coastal plains have high socio-economical value due to the presence of a high concentration of infrastructures (highway, roads, railways, etc.), industrial and urban areas. Several touristic activities are mainly located nearby the coastline and provide a high employment ratio, especially during the summer season. Numerous agricultural and livestock farms are located in the inner sector of the plain forming the main economic activities supporting the local economy during the whole year. Finally, these areas are also characterized by high environmental and archaeological values to the presence of protected natural areas and relevant archaeological sites (i.e., Paestum remains).

## Methods

To assess the future scenarios of coastal inundation risk, a three-step methodology is here proposed (as shown in the flow chart in Fig. 2):

Step 1—Proneness analysis: the low topographic areas are identified and classified in four hazard classes of inundation accounting for expected local sea levels, following a modified classification proposed in Aucelli et al. (2017a, 2018) and Di Paola et al. (2018). To this aim, relative sea levels for the years 2065 and 2100 are evaluated as a combination of sea-level projections proposed by IPCC (2014) and local vertical displacement rates estimated by Multi-Temporal Synthetic Aperture Radar Interferometry (MT-InSAR) data analysis (Matano 2019).

Step 2—Exposure analysis: the anthropic and natural elements located in the areas prone to be impacted by sea-level rise as well as the social vulnerability level of the coastal communities are identified and classified in four classes of exposure level (following the methodological approach proposed in Rizzo et al. 2020).

Step 3—Risk assessment: once the hazard and the exposure classes have been identified (Step 1 and Step 2), the inundation risk is calculated by combining these layers and classified the investigated areas in four risk classes (ranging from R1- low risk, to R4 – high risk), as already proposed in several studies (Benassai 2015; Aucelli et al. 2017a, 2018; Di Paola et al. 2018).

In the following subparagraphs, each step and the required data needed for the analysis are described in detail.

### Step 1: Proneness Analysis

#### Vertical Ground Deformation Movements (VGDMs) evaluation

The assessment of VGDMs is carried out by analyzing the MT-InSAR datasets available for the study areas. In details, Italian national and regional remote sensing projects (Regione Campania 2009a, b; EPRS 2015) have produced several processed datasets referred to both ascending and descending orbits, by radar images acquired by C-band sensors on-board ERS-1/2, ENVISAT and RADARSAT satellites (Table 1). These datasets, referred to about two decades (1992–2010) overall, have been implemented with different processing methods, such as Permanent Scatterometers (PS-InSAR) (Ferretti et al. 2001, 2007) and Persistent Scatterometers Pairs (PSP) (Costantini et al. 2009). For those areas common to both acquisition satellite geometries, the availability of coeval datasets from a different point of view allows for the evaluation of the vertical components of the ground deformation, based on the interpolation of Permanent Scatterometer Interferometry (PSI) point data and some trigonometric calculations (Vilardo et al. 2009; Matano 2019). The obtained 50-m spaced grid maps show the distribution of the vertical components of ground deformation velocity in the studied coastal plains related to 1992–2000

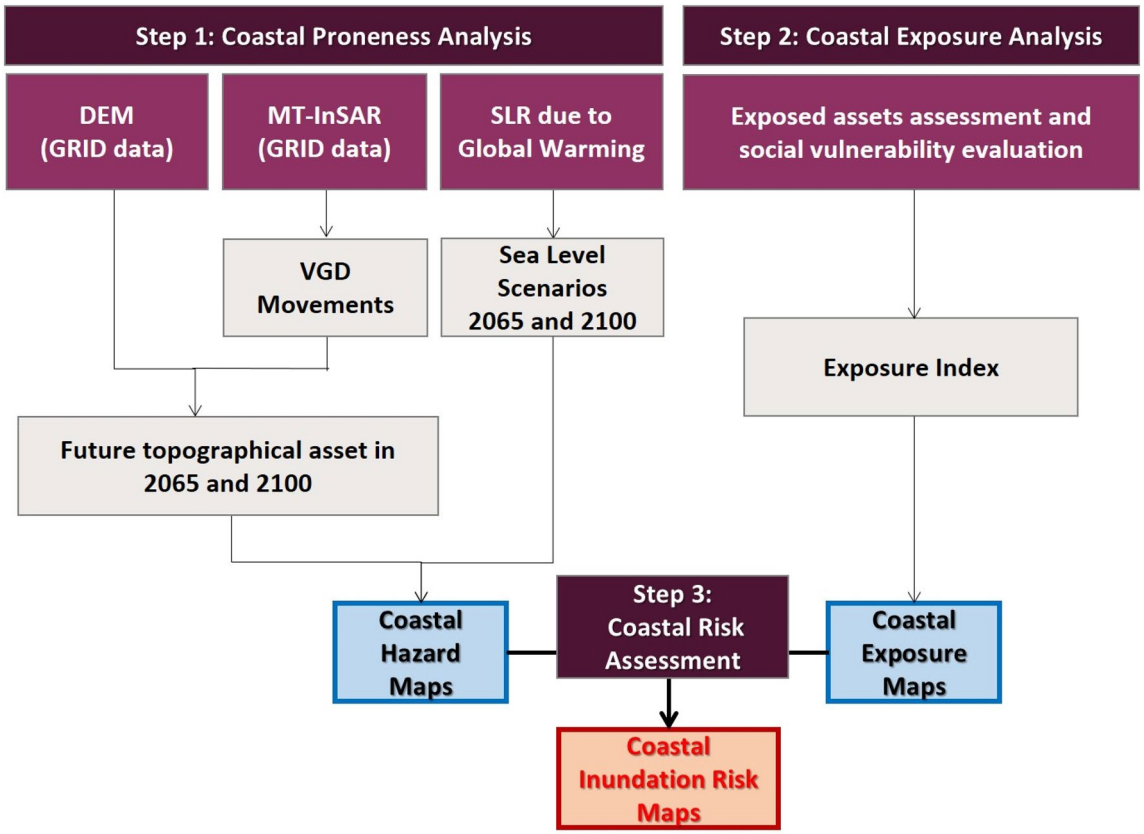


**Fig. 2** Coastal inundation risk analysis. The methodology proposed for the evaluation of the coastal inundation risk is composed of three steps of analysis, which are aimed at: evaluating of the proneness of the coastal areas to sea-level impacts (Step 1); evaluating of the exposure level (Step 2); evaluation of the overall risk (Step 3)

**Table 1** Satellite data. Main information related to the PSI data used for the assessment of the VGDM rates

| Satellite (Orbit) | PS technique | Data Source | LOS | Time range |
|---|---|---|---|---|
| ENVISAT (Ascending) | PSP | EPRS-E (MATTM) | 22° | Nov. 2002 – Jul. 2010 |
| ENVISAT (Descending) | PSP | EPRS-E (MATTM) | 25° | Nov. 2002 – Jun. 2010 |
| RADARSAT (Ascending) | PS-InSAR | TELLUS Project (Regione Campania) | 34° | Mar. 2003 – Sep. 2007 |
| RADARSAT (Descending) | PS-InSAR | TELLUS Project (Regione Campania) | 32.5° | Mar. 2003 – Aug. 2007 |
| ERS-1/2 (Ascending) | PSP | EPRS-E (MATTM) | 22° | Jun. 1992 – Jan. 2001 |
| ERS-1/2 (Descending) | PSP | EPRS-E (MATTM) | 23° | Jun. 1992 – Dec. 2001 |

(ERS-1/2 dataset), 2003–2007 (RADARSAT dataset) and 2003–2010 (ENVISAT dataset). To obtain a quantitative assessment of the subsidence process, the average rates of Vertical Ground Deformation Movements (expressed in mm/year) were calculated for the whole period 1992–2010 with a weighted average (Matano 2019).

## Future Relative Sea Level Rise (RSLR) scenarios

The local sea-level projections are calculated by combing global scenarios with local VGDMs to evaluate the RSLR for the investigated coastal sectors (as already done in Antonioli et al. 2017, 2019). Based on the assumption that the

present subsidence trends will be constant in the next decades (Aucelli et al. 2017a), local VGDMs rates are used to obtain the future component of relative variation in sea level. To have two scenarios for short and long term, the analysis is carried out taking into the mean values of global sea-level projections relative to 2046–2065 and 2100 (vs 1986–2005) proposed by the IPCC in the last Assessment Report (AR5, 2014). Furthermore, to represent the most likely scenario, the worst Representative Concentration Pathway scenario (RCP8.5) has been considered (Table 2).

### Coastal Inundation Hazard Analysis

Based on the criteria that the areas potentially prone to be inundated as consequences of RSLR are those areas lying either below sea level or less elevated above it, the coastal inundation hazard analysis is carried out by investigating the topography of the study areas, provided by the Italian Environment Ministry (MATTM 2017), who carried out a LiDAR survey in 2012 producing a DEM with 1 m pixel. To this purpose, the GIS-based "bathtub approach" is used to identify areas below the future sea levels, and four classes (from H1 to H4) hazard classification (Aucelli et al. 2017a) is applied. The hazard zonation is based on different proneness level of the coastal territory and accounts for the potential coastal response. In detail, H1 includes areas prone to be inundated only occasionally, (usually located above 1 m a.s.l.), classes H2 and H3 identify areas that are prone to frequent inundation events and permanent morphological changes, such as beach and dune erosion. Finally, class H4 identifies areas prone to be permanently inundated because below the current mean sea level (Table 3). The inland limit for the inundation analysis has been set at 5 m a.s.l., as proposed in the frame of EUROSION Project (2004).

**Table 2** Sea-level projections

| Scenario | Year | Sea-level rise (m) |
|---|---|---|
| IPCC RCP8.5 | 2046–2065 | 0.30 |
| | 2100 | 0.74 |

Mean values of global mean sea-level rise in 2041–2065 and 2100 relative to 1986–2005 under the RCP8.5 scenario (from IPCC, 2014)

### Step 2: Coastal Exposure Analysis

To assess the anthropic assets located in the zones prone to be inundated, an index-based methodology is proposed. The method follows the index approach suggested in previous studies and applied in different coastal areas (Rizzo et al. 2020; Aucelli et al. 2018; Armaroli and Duo 2017; Ferreira et al. 2017; Viavattene et al. 2015), which assumes that the exposure can be represented by a set of socio-economic indicators: land use categories, transport networks, utilities and business settings. Furthermore, the social vulnerability of the municipalities is also taken into account. Sources of exposure data used in this study are reported in Table 4. As for the hazard analysis, the landward limit of the analysis has been set at 5 m a.s.l.

The Land Use indicator (Exp_LU) measures the relative exposure of each land use category, after having grouped them in five classes according to an anthropocentric perspective (Ballesteros et al. 2018; Perini et al. 2016). This classification defines as very highly exposed areas the ones occupied by settlements, constructions and human activities, corresponding to the "Artificial surfaces" class (Corine Land Cover—Level 1) while assigns a very low exposure level to the natural areas and the inland water courses, corresponding to the "Water Bodies" class (Corine Land Cover—Level 1). This indicator considers the presence of a given "land use category" and the associated relative importance value but not its physical vulnerability. Nevertheless, natural protected areas (Nature 2000 sites) are considered as highly vulnerable.

**Table 3** Hazard classes. Inundation hazard classes with the corresponding ranges and the potential coastal response (after Aucelli et al. 2018)

| Hazard classes | Topographical Range | Coastal system response |
|---|---|---|
| H4 | Height ≤ 0 m | Permanent marine inundation<br>Area expected to be in the future below the mean sea level and therefore very prone to be permanently inundated |
| H3 | 0 m < height ≤ 0.5 m | Potential inundation and morphological response<br>Area prone to frequent events of temporary flooding due to a combination of sea storms and/or fluvial actions and characterized by permanent morphological changes due to erosion and sedimentation |
| H2 | 0.5 m < height ≤ 1 m | Morphological response and low potential inundation<br>Area prone to flooding due to combination of sea storms and/or fluvial actions and characterized by low permanent morphological changes |
| H1 | 1 m < height ≤ 5 m | Very low potential inundation<br>Area prone to be temporarily flooded only due to high energy sea storms and/or fluvial actions |

**Table 4** Coastal exposure index. Indicators proposed for the evaluation of the exposure index and related sources

| Coastal Exposure Index | | |
|---|---|---|
| Code | Indicator | Data |
| Exp_LU | Land use category | Corine Land Cover map (2012) http://land.copernicus.eu/ |
| Exp_Tr | Transport networks | Photointerpretation (Google Earth images 2014) and regional data (CTR 2004) |
| Exp_Ut | Utilities | Territorial local coordination plans (Città Metropolitana di Napoli 2015; Provincia di Caserta 2009; Provincia di Salerno, 2012) |
| Exp_Bs | Business setting | Photointerpretation (Google Earth images 2014) |
| Exp_SVu | Social vulnerability | Social vulnerability index (ISTAT, 2011) http://ottomilacensus.istat.it/ |

The Transport networks indicator (Exp_Tr) is ranked according to the importance of the transport system within its network. The lowest value is attributed to local roads, the highest one, instead, to roads and railways of national or international importance. The potential area of competence of each element of the transport network has been set within a buffer of 150 m along their central line.

The Utilities indicator (Exp_Ut) is evaluated based on the presence of electricity stations and water supply plants, which are considered very critical assets. The potential area of competence of each asset has been set as a buffer of 100 m around them.

The Business indicator (Exp_Bs) considers the presence of bathing establishments located along the coastline because bathing tourism represents one of the main economic activities along these coasts. The potential area of competence has been set as a buffer of 200 m from the coastline.

Transport networks, utilities and business settings are the three indicators used to evaluate the anthropic assets located in the investigated coastal areas.

Detailed information about the classification of each exposure indicator is reported in Table 5.

The Social Vulnerability indicator (Exp_SVu) measures the relative vulnerability of the different communities located along with the coastal sectors. This indicator allows evaluating the socio-economic characteristics of the population exposed to coastal hazards and it is generally obtained from census data. For the Italian case, this indicator is expressed by an index defined and calculated for the whole Italian territory by the National Statistical Institute (ISTAT).

The Italian Social-vulnerability index is calculated at the municipality level and it is constructed through the synthesis of seven indicators that account for the following aspects: family structure (number and age of family members, young single-parent families), living condition, labor market participation, and percentage incidence of households with

**Table 5** Coastal exposure indicators and their classification.

| Exposure indicator | Exposure level | | | | |
|---|---|---|---|---|---|
| | Very low (1) | Low (2) | Moderate (3) | High (4) | Very High (5) |
| Land use | Inland waters bodies | Wetland, Lagoon and no vegetated areas | Forest, Beaches, Dune | Agricultural areas | Urban, Industrial and protected natural areas (SCI) |
| Transport network | Absence of road network | Road network of local importance | Road network of regional importance | Road network of national importance | Train network and Highway |
| Utilities | Absence of utilities network | Utilities network of local importance | Utilities network of regional importance | Electricity grid/ aqueduct of regional importance | Utilities network of national importance |
| Business | Absence of summer concessions | – | – | – | Presence of summer concessions |
| Social Vulnerability (ISTAT index*) | 93.6 – 96.69 | 96.7 – 99.79 | 99.8 – 102.89 | 102.9 – 105.99 | 106—109 |

potential economic and welfare distress. The selected indicators describe, with almost equal weight, the two dimensions of "material" and "social" vulnerability. The operative ISTAT procedure is described in detail at the following link:

http://ottomilacensus.istat.it/fileadmin/download/Indice_di_vulnerabilit%C3%A0_sociale_e_materiale.pdf

The Coastal Exposure is calculated by the geometric mean of the listed indicators, defined as the nth root of the product of n indicators (Eq. 1). The obtained Coastal Exposure Index is converted into a scale from 1 (low exposure) to 4 (very high exposure) (Table 5).

$\mathbf{Exposure}_{\mathbf{Index}} = [\mathrm{Exp\_LU} * (\mathrm{Exp\_Tr} + \mathrm{Exp\_Ut} + \mathrm{Exp\_Bs}) * \mathrm{Exp\_SVu}]^{1/3}$ (Eq. 1).

### Step 3: Coastal Inundation Risk Analysis

The inundation risk is defined as the combination of the probability of the hazardous event and its negative consequences (impacts). It is calculated by means of the risk matrix (Table 6) proposed in Aucelli et al. (2017a) and classified in the following four classes:

R4 (very high risk): permanent loss of the current socio-economical activities; disruption of structures, infrastructures and relevant areas.

R3 (high risk): high damage of the current socio-economical activities; potential loss of structures, infrastructures and relevant areas.

R2 (medium risk): medium damage to the current socio-economical activities.

R1 (low risk): low damage to the current socio-economical activities.

## Results

### Coastal inundation hazard assessment

The results of the quantitative assessment of the subsidence process referred to the four studied coastal plains are showed in 50-m spaced grid maps (Fig. 3), displaying the average rates of Vertical Ground Deformation Movements (expressed in mm/year) referred to the period 1992–2010. These maps show that the coastal sector of the Volturno and Sele plains are characterized by complex subsidence patterns, resulting in more intense and wider than those characterizing Sarno and Alento plains.

In detail, the Volturno River mouth is characterized by moderate subsidence values (-2.5 to -7.5 mm/y), while the dune ridge system shows low subsidence (0 to -2.5 mm/y). High subsidence values (up to -10 mm/y) are found in the back-dune depressions, near Lago Patria Lake and Villa Literno town. The central part of the Volturno Plain, in the Cancello Arnone surrounding area, displays subsidence values ranging from -2.5 to -20 mm/y. The Sele River mouth area is characterized by moderate values of subsidence (-2.5 to -7.5 mm/y) with a hot spot developing 5 km inland. In the northern sector, a continuous coastal strip is characterized by subsidence values ranging between -2.5 and -10 mm/y, while the hilly areas towards the east and the southern sector of the plain are characterized by general condition of stability.

The Sarno coastal plain is characterized by localized moderate subsidence near Castellammare di Stabia ( -0.25 to -1 mm/y) and high subsidence rates (-1 to -5 mm/y) near the river mouth. In the strip between 1 and 2 km inland the coastline, the ground shows stability trend (-0.25 to +0.25 mm/y). Along the inner alluvial plain, strong subsidence affects the area close to the Sarno River around the city of Santa Maria La Carità. The Alento plain shows a moderate pattern of vertical ground deformation. The northern sector shows low subsidence rates (-1.9 to -0.3 mm/y) and the coastal narrow strip among Velia and Marina di Ascea displays stability or fair uplift ( -0.3 to +0.6 mm/y), while 1–2 km inland along the Alento River course, a hot spot of subsidence is evident (up to -3 mm/y).

The area characterized by each hazard class has been evaluated for all the investigated coastal plains considering the RCP8.5 scenario for the years 2065 and 2100. In details, a total surface of approximately 180 $km^2$ (Volturno Plain), 8.5 $km^2$ (Sarno Plain), 60 $km^2$ (Sele Plain), 7 $km^2$ (Alento Plain) has been investigated. The detailed extent of each hazard class is shown in Table 7; values are expressed both as square kilometers and as percentage.

Considering the 2065 projections (Fig. 4), the extent of H4 class is relevant only for the Volturno plain (38.2 $km^2$ corresponding to 21% of the total investigated area) while, for the others studied coastal plains, it extends less than 10% with the lowest value estimated for the Alento plain (< 1%). Also, H3 and H2 classes extend, respectively, 11% and 13% in the Volturno plain and with a percentage lower than 10% for the other coastal plains. Accounting for H1 class, its surface occupies 94% of the investigated area in the Alento

**Table 6** Coastal risk matrix. The risk is evaluated by combining the coastal Hazard level (H) with the exposure level (Ex). The different colors evidence the different risk classes ranging from low in green (R1) to very high in red (R4). From Aucelli et al. (2017a)

| Risk | | Exposure | | | |
|---|---|---|---|---|---|
| | | $E_x4$ | $E_x3$ | $E_x2$ | $E_x1$ |
| Hazard | H4 | R4 | R4 | R3 | R2 |
| | H3 | R4 | R3 | R2 | R1 |
| | H2 | R3 | R2 | R2 | R1 |
| | H1 | R2 | R1 | R1 | R1 |

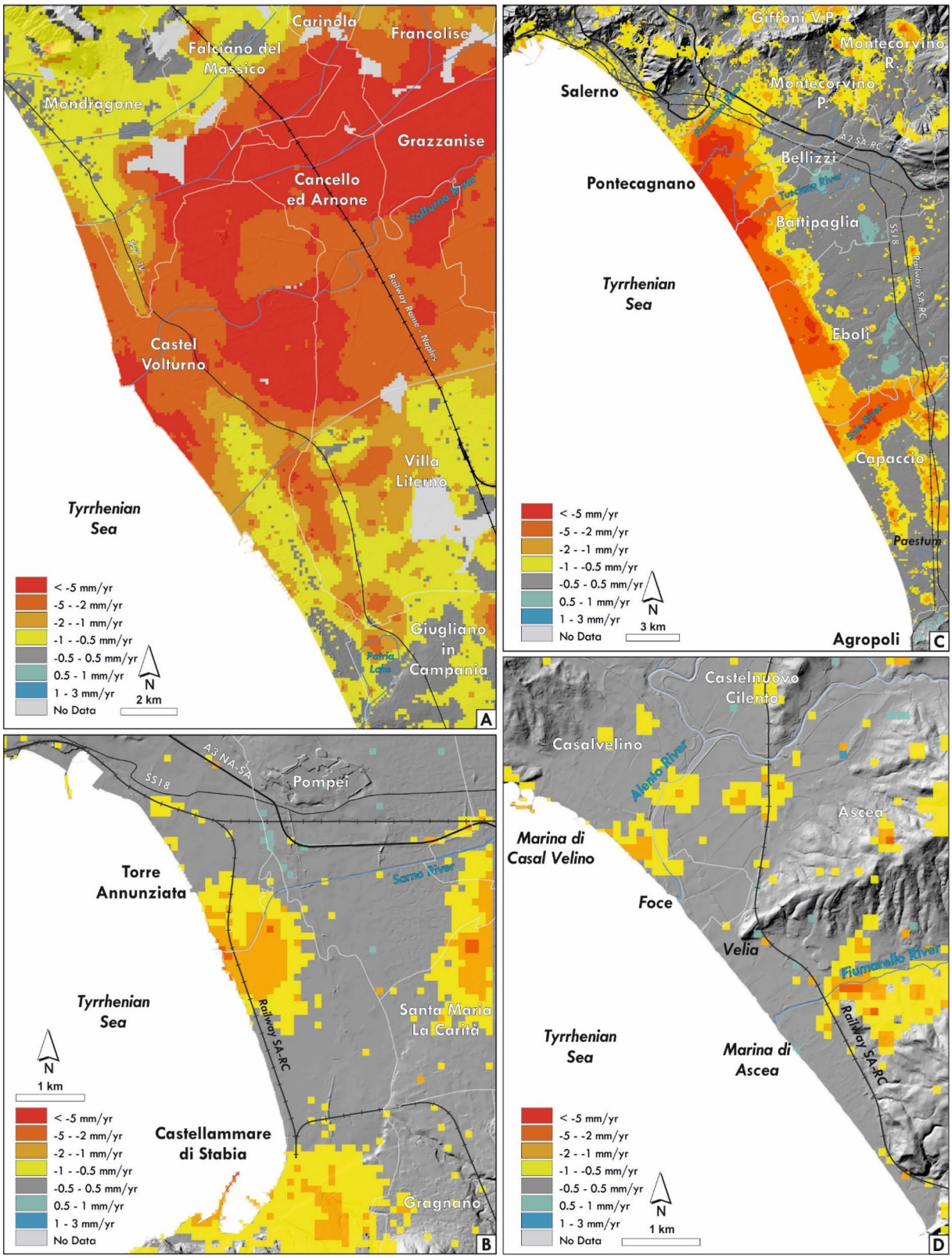


**Fig. 3** – Local Vertical Ground Deformation Movements maps for the studied coastal plains. Volturno coastal plain (**A**), Sarno coastal plain (**B**), Sele coastal plain (**C**), Alento coastal plain (**D**)

**Table 7** Coastal inundation hazard assessment. The surface of each hazard class is indicated as square kilometers and percentage of the total investigated surface by considering sea-level rise scenarios for the years 2065 and 2100 (RCP8.5). For the hazard class rank, refer to Table 3

| | SCENARIO (RCP8.5) | H1 ($km^2$/%) | H2 ($km^2$/%) | H3 ($km^2$/%) | H4 ($km^2$/%) |
|---|---|---|---|---|---|
| Volturno Plain | 2065 | 98.4/54.6 | 24.0/13.3 | 19.6/10.9 | 38.2/21.2 |
| | 2100 | 76.4/42.3 | 19.9/11.0 | 22.8/12.6 | 61.6/34.1 |
| Sarno Plain | 2065 | 7.8/92.3 | 0.4/4.2 | 0.1/1.5 | 0.2/2.0 |
| | 2100 | 7.4/83.7 | 0.8/9.4 | 0.3/3.8 | 0.3/3.1 |
| Sele Plain | 2065 | 45.6/75.8 | 6.3/10.4 | 4.2/7.1 | 4.0/6.7 |
| | 2100 | 38.1/63.0 | 7.5/12.0 | 6.3/10.0 | 8.7/14.0 |
| Alento Plain | 2065 | 6.4/94.1 | 0.2/2.5 | 0.2/2.5 | 0.1/0.9 |
| | 2100 | 5.9/86.2 | 0.6/8.3 | 0.2/2.4 | 0.2/3.2 |

Plain, 92% in the Sarno Plain, 76% in the Sele Plain and 55% in the Volturno Plain. Considering the 2100 projections (Fig. 5), the extent of H4 class in the Volturno Plain is 61.6 $km^2$ and 8.7 $km^2$ in the Sele Plain (34% and 14% of the total investigated area, respectively), while for the others investigated coastal plains, the H4 surface is less than 3%. H3 and H2 classes occupy, respectively, 22.8 $km^2$ (13%) and 19.9 $km^2$ (12%) in the Volturno Plain. Also, in this case, these classes have a surface than 10% in the other coastal plains. Finally, the H1 class surface decreases in all the plains with passing to 86% in the Alento Plain, 84% in the Sarno Plain, 63% in the Sele Plain and 42% in the Volturno Plain.

### Negative rates show subsidence, positive rates uplift

### Coastal exposure assessment

The exposure evaluation (Fig. 6) has accounted for the current spatial distribution of the vulnerable assets and social vulnerability. Results are shown in Table 8 both in $km^2$ and as a percentage of the investigated area for each plain.

Results show that Class Ex3 has the highest values almost in all the investigated plains, corresponding to 83% (Alento), 50% (Volturno), 45% (Sele), and 31% (Sarno) of the total surface. Class Ex4 has the highest percentage value in the Sarno Plain (68%), while it occupies 44% of the investigated area in the Volturno Plain and 8.4% in the Sele Plain.

### Coastal inundation risk assessment

To assess the spatial distribution of the different risk levels along the investigated coastal plains, the hazard and the exposure classes have been combined following the coastal risk matrix (Table 6). Risk has been classified in four classes and the results are shown as risk maps to each plain (Fig. 7 and Fig. 8). Furthermore, the extent of each class risk is indicated in Table 9, where the results are shown in $km^2$ (a) and as percentage values (b).

Accounting for the R4 class, it has a considerable extension only in the Volturno Plain (48.9 $km^2$ and 73.7 $km^2$, respectively, in 2065 and 2100 scenario) and in the Sele Plain (2.8 $km^2$ and 6.1 $km^2$, respectively, in 2065 and 2100 scenario). In the other investigated coastal plains, R4 class extends for a limited surface (lower than 2% of the total areas). Class R3 has an extension of more than 11% only in the case of Volturno plain. R1 class shows the largest areas in Sele, Volturno and Alento Plains for both considered time-periods, while R2 class occupies the largest surface in Sarno Plains.

In Table 10 R4 and R3 classes areas are shown, referred to 2065 and 2100 scenarios on a municipality basis. The municipalities located in the Volturno Plain show high values of R3 and R4 areas in both scenarios. In particular, the Castel Volturno, Villa Literno and Mondragone municipalities show high values of R4 in 2100 (37.0 $km^2$ – 50.1%) and R4 in 2065 (20.8 $km^2$ – 32.1%). Within the other plains, the only municipality with relevant values of R4 areas is Eboli in the Sele Plain (2.5 $km^2$ – 1.8% in 2065 and 5.5 $km^2$ – 4.0% in 2100).

## Discussion and conclusion

The analysis of sea-level rise impact along the Campanian coastal plains has provided a detailed mapping of the coastal areas prone to be impacted by sea inundation for the years 2065 and 2100. In addition, risk scenarios suggest that in the next decades, natural areas, including beaches and wetland, human infrastructures, and touristic areas as well as wide portions of agricultural areas can be affected by marine inundation and related impacts.

In detail, the results of the hazard assessment have shown that considering the RCP8.5 scenario, the total surface of H4 class is expected to be 42.5 $km^2$ and 70.8 $km^2$ in the year 2065 and 2100, respectively. Taking into account the increase in H4 surface from 2065 to 2100, the maximum value is calculated for the Volturno coastal plain, where it increases of 23.4 $km^2$ (+13%), passing from 38.2 to 61.6 $km^2$, while the lowest value has been estimated for the Sarno coastal plain where it increases only 0.1 $km^2$ (+1.3%), passing from 0.1 to 0.2 $km^2$. In the case of the Sele coastal plain, this value increases 4.7 $km^2$ (+7.3%) while in the Alento coastal plain, the increasing in H4 surface is 2.3%.

From these results, it is clear that the observed subsidence trends play a consistent role in increasing sea-level rise impact along the investigated coastal stretches, especially in the Volturno coastal plain, where current subsidence rates

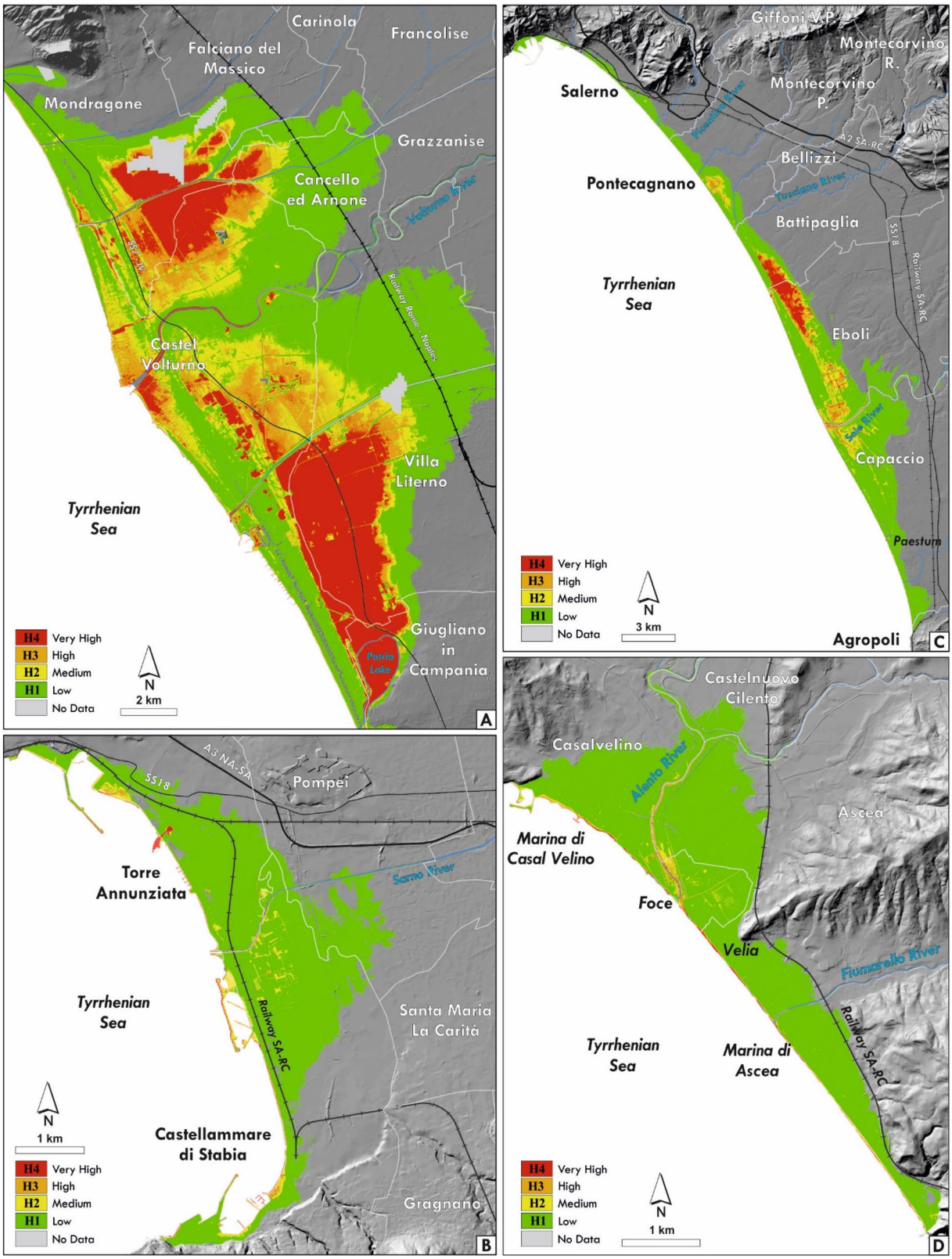


**Fig. 4** Inundation hazard maps for the year 2065 (under the RCP8.5 scenario). Volturno coastal plain (**A**), Sarno coastal plain (**B**), Sele coastal plain (**C**), Alento coastal plain (**D**)

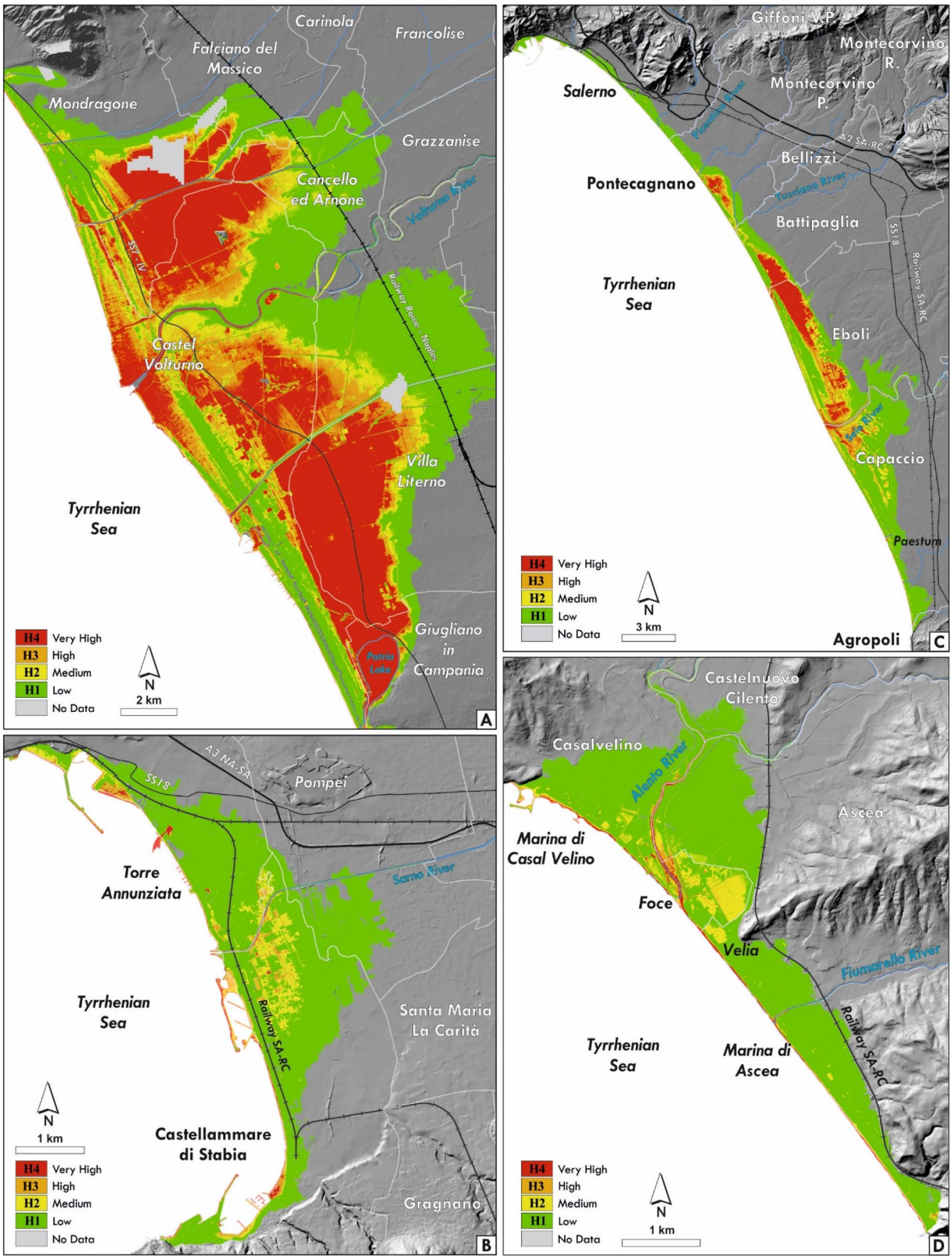


**Fig. 5** Inundation hazard maps for the year 2100 (under the RCP8.5 scenario). Volturno coastal plain (**A**), Sarno coastal plain (**B**), Sele coastal plain (**C**), Alento coastal plain (**D**)

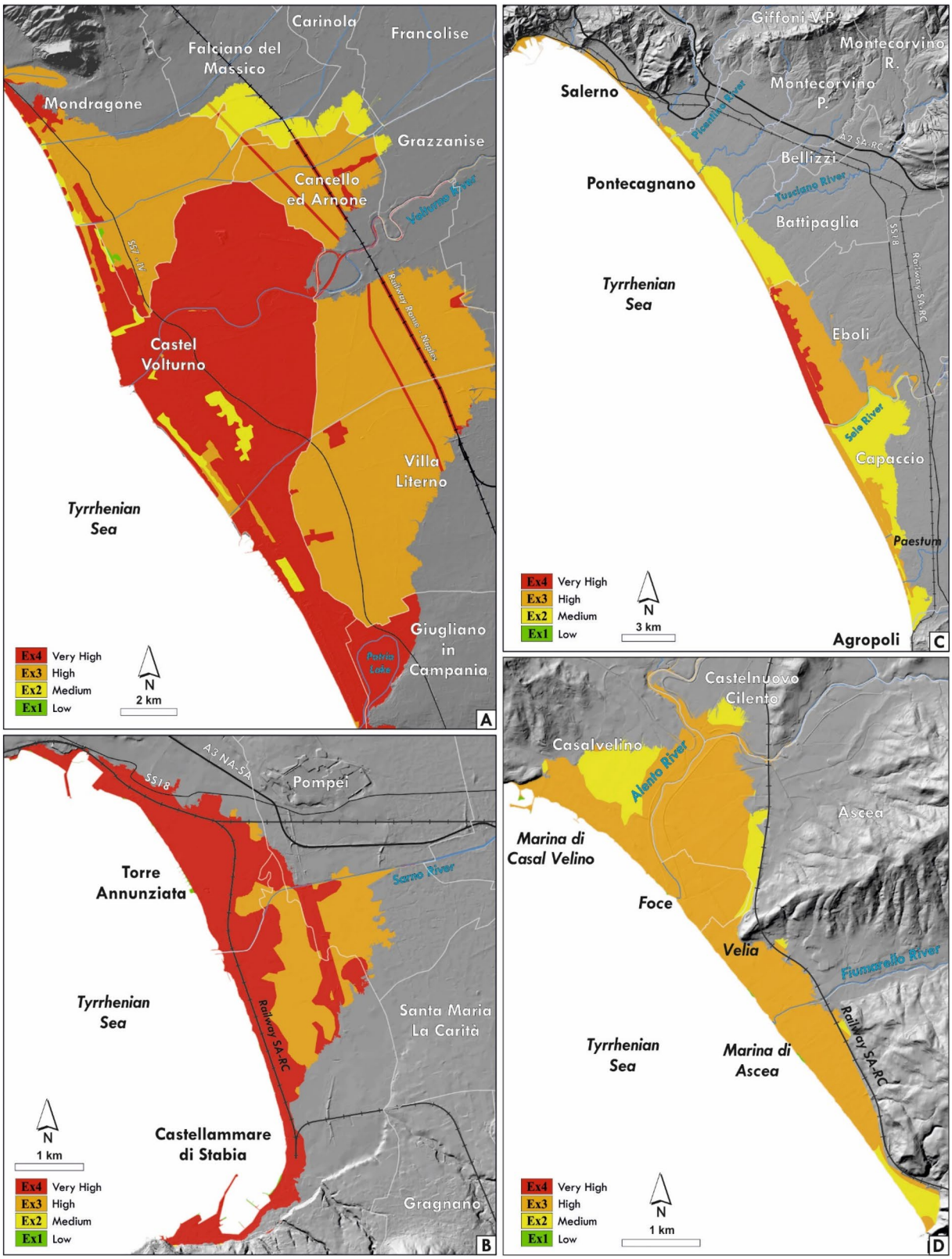


**Fig. 6** Exposure maps. Volturno coastal plain (**A**), Sarno coastal plain (**B**), Sele coastal plain (**C**), Alento coastal plain (**D**)

**Table 8** Coastal exposure assessment. The surface of each class is indicated as square kilometers and percentage of the total investigated surface

| | *Ex1* $km^2$/% | *Ex2* $km^2$/% | *Ex3* $km^2$/% | *Ex4* $km^2$/% |
|---|---|---|---|---|
| Volturno Plain | 1.2/0.1 | 9.7/5.2 | 95.0/50.4 | 83.3/44.3 |
| Sarno Plain | 0.1/0.4 | -/- | 2.7/31.3 | 5.9/68.3 |
| Sele Plain | 0.5/0.9 | 27.6/45.8 | 27.1/44.9 | 5.1/8.4 |
| Alento Plain | 0.1/0.2 | 1.2/17.0 | 5.7/82.8 | -/- |

range from -1 to -25 mm/yr and the H4 class reaches its maximum extend, and in the Northern sector of the Sele coastal plain. Due to the geological setting of these plains, the detected high subsidence can be considered mainly a natural process caused by the compaction of the alluvial sediments infill under the lithostatic load (Ruberti et al. 2017; Aucelli et al. 2017a; 2018; Di Paola et al. 2018; Matano et al. 2018; Amato et al. 2020). Conversely, anthropic influences (e.g., water pumping and urbanization) are considered as an additional factor that may locally increase the natural subsidence processes.

Accounting for the risk analysis, results have shown that 51.9 $km^2$ are including in the R4 class in 2065. This value will increase up to 80.3 $km^2$ when the scenario for the year 2100 is taken into account. Also in this case, the maximum surface increasing from 2065 to 2100 is expected to occur in the Volturno and Sele coastal plains, with increasing values of + 13.7% and + 5.5%, respectively.

The proposed methodological approach is consistent with several types of research that have been carried out for mapping areas that will be impacted by sea-level rise as a consequence of global warming and local subsidence. In fact, a number of recent international studies focused on the definition of risk management and adaptation strategies tailored accounting for the small-scale criticalities highlighted by high-resolution information obtained by coupling MT-InSAR subsidence maps with expected sea levels. By way of example, an increase of 25% in the potentially flooding surface in the central Singapore zone is expected by 2100 as consequence of local subsidence (Catalao et al. 2020). Local subsidence will exacerbate inundation risk also in the San Francisco Bay, where analysis results show that inundation hazard scenarios based only on the projection of sea-level rise may underestimate the area at flooding risk. In details, considering the lower and upper bounds of likely ranges of various RCP-projected SLR scenarios coupled with local subsidence trends, in 2100, an area of 98 to 218 $km^2$ will be affected by RSLR. The corresponding values for the case of SLR only are 51 to 168 $km^2$ (Shirzaei & Bürgmann 2018a, b). Another example is provided by Le Cozannet et al. (2021), who have analyzed the Guadeloupe area (West Indies, French Antilles). This coastal area is characterized by local subsidence mainly caused by changes in the water content of reclaimed ground and strong urbanization occurring since the 1950', which is causing high sediment compaction. Also in this case, future chronic flooding events are expected to be exacerbated by land subsidence. In Italy, Antonioli and Silenzi (2007), Lambeck et al. (2011), Antonioli et al. (2017; 2020) proposed a first level of assessment of the impacts of future relative sea levels at a regional scale along the main Italian coastal plains, which are characterized by different geological settings and tectonic movements. Nevertheless, in these studies, the ground deformation processes have been evaluated only for large homogeneous sectors on the basis of geological proxies and constrain. Data with a more accurate and detailed spatial resolution of the local vertical ground movements obtained using Multi-Temporal SAR Interferometry datasets represent a great benefit for the risk assessment allowing to discriminate areas that are affected by different subsidence rates both along the waterfront sectors and in the inland low-lying areas. Similar analysis have been carried out along other Italian coastal sectors. Recently, Anzidei et al. (2021) have evaluated the impact of relative sea-level scenario in 2100 along the Coast of South Eastern Sicily (Italy) using MT-InSAR data, satellite images and high-resolution topography. In this case, a total surface of approximately 10 $km^2$ is expected to be flooded in 2100 under the RCP8.5 scenario, with a marine ingression up to 5 km inland in the Catania coastal area, due to the local complex topographical characteristics.

The results of our study represent a step forward with respect to the findings of previous works published on the Volturno and Sele coastal plains (Aucelli et al. 2017a, b; Di Paola et al. 2018), extending the hazard analysis to all the Campania region coastal plains and defining a uniform risk analysis procedure to be applied in all the investigated coastal plains. This last aspect highlights an important outcome of this work that has enabled the relative ranking of the main Campanian coastal plains in terms of inundation risk. These kinds of studies increase the awareness of the communities that will have to deal with permanent sea ingression, which will force them to find strong adaptation strategies to cope with its potential impacts and to preserve the economic and natural values of the assets potentially impacted. Therefore, this analysis gives a useful instrument to local administrations to evaluate in detail areas to be strictly monitored to avoid loss of goods. In spite of its simplified approach, this work represents a useful instrument for planner authorities and the necessary preliminary step for the identification of the coastal sectors that require to be investigated in more

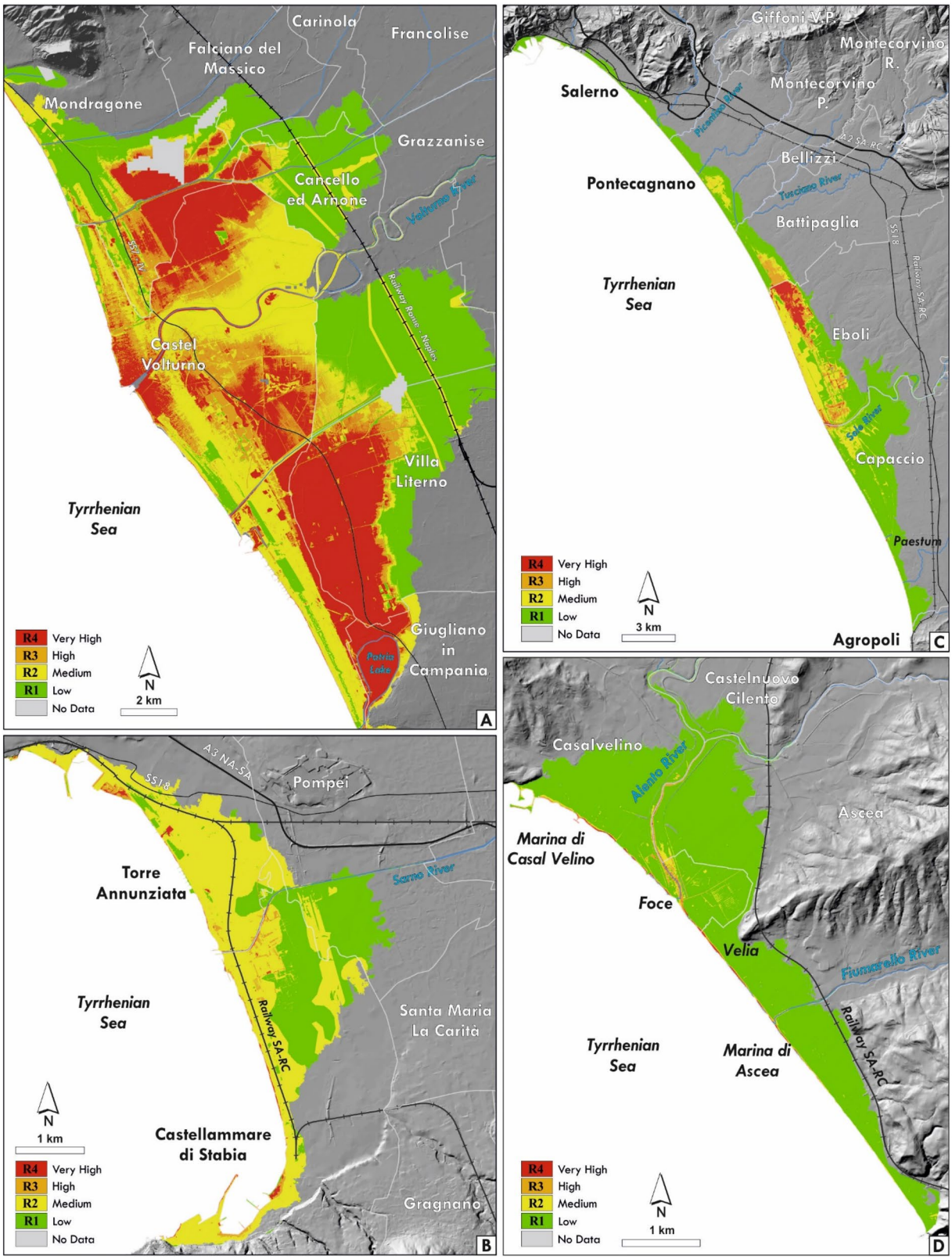


**Fig. 7** Inundation risk maps for the year 2065 (under the RCP8.5 scenario). Volturno coastal plain (**A**), Sarno coastal plain (**B**) Sele coastal plain (**C**), Alento coastal plain (**D**)

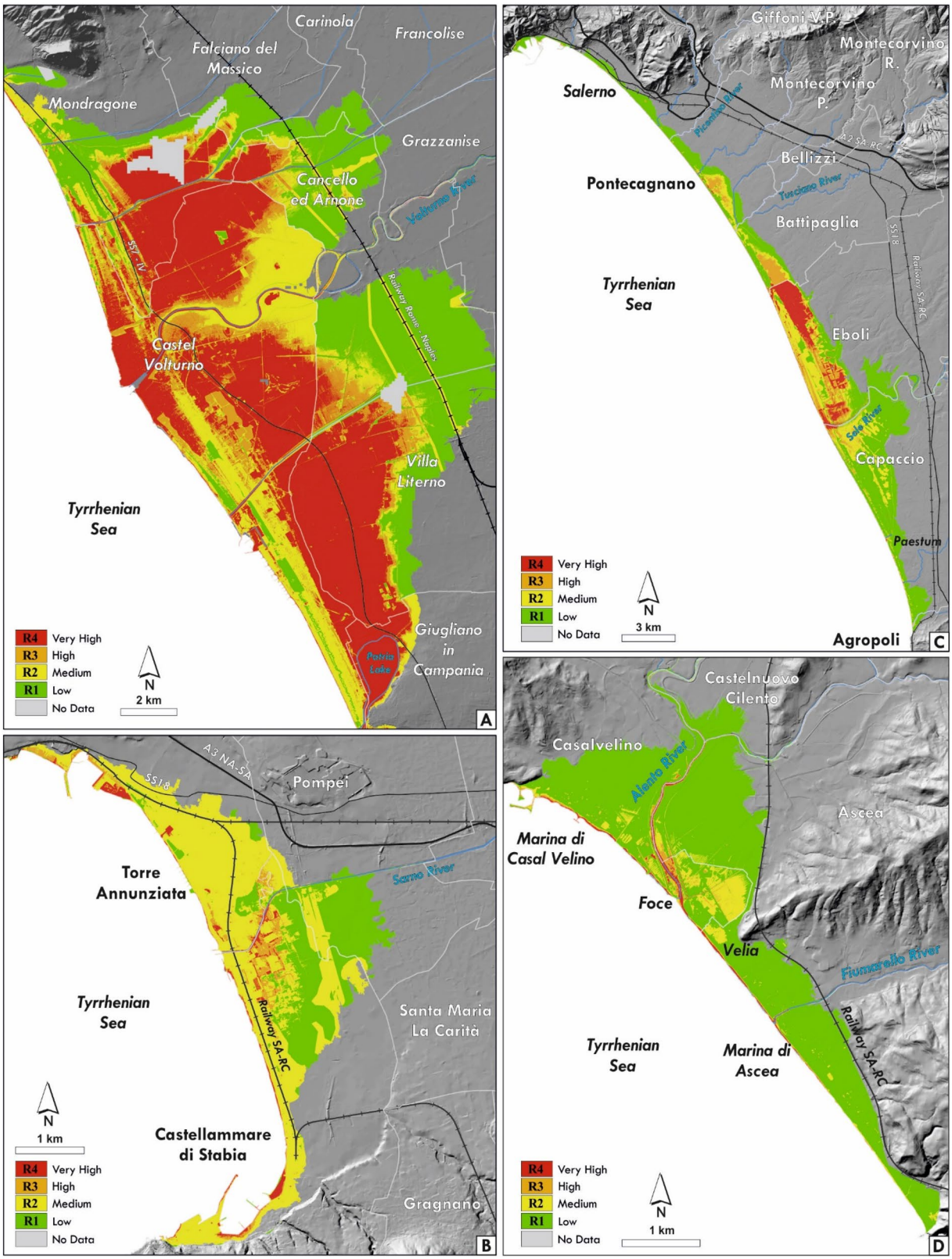


**Fig. 8** Inundation risk maps for the year 2100 (under the RCP8.5 scenario). Volturno coastal plain (**A**), Sarno coastal plain (**B**) Sele coastal plain (**C**), Alento coastal plain (**D**)

**Table 9** Coastal inundation risk assessment. The surface of each risk class is indicated as square kilometers and percentage of the total investigated surface by considering sea-level rise scenarios for the years 2065 and 2100 (RCP8.5) and the present distribution of exposure classes

| | *SCENARIO (RCP8.5)* | *R1 ($km^2$/%)* | *R2 ($km^2$/%)* | *R3 ($km^2$/%)* | *R4 ($km^2$/%)* |
|---|---|---|---|---|---|
| Volturno Plain | 2065 | 60.3/33.2 | 48.9/27.0 | 23.4/12.9 | 48.9/26.9 |
| | 2100 | 50.7/27.9 | 36.5/20.1 | 20.7/11.4 | 73.7/40.6 |
| Sarno Plain | 2065 | 2.9/34.4 | 5.3/61.6 | 0.2/2.7 | 0.1/1.3 |
| | 2100 | 2.5/28.9 | 5.2/61.3 | 0.5/6.0 | 0.3/3.8 |
| Sele Plain | 2065 | 41.8/69.6 | 11.4/18.9 | 4.1/6.9 | 2.8/4.6 |
| | 2100 | 34.7/57.7 | 12.6/21.0 | 6.7/11.2 | 6.1/10.1 |
| Alento Plain | 2065 | 6.4/94.7 | 0.2/2.5 | 0.2/2.2 | 0.1/0.6 |
| | 2100 | 5.9/86.7 | 0.6/8.5 | 0.2/2.2 | 0.2/2.6 |

detail by means of higher resolution and dynamic modeling approaches.

In detail, the hazard and risk inundation maps here proposed can represent a tool for increasing efficient territorial management aimed at the reduction of future coastal risk. In fact, up till now, the coastal management plans provided by the regional Authorities are drawn up according to the national regulations, which suggest mapping coastal erosion and flooding scenarios by considering only the impact of storm surges with different return periods without considering the potential contribution of subsidence processes.

The risk assessment procedure applied in this study allows obtaining a coastal zonation that accounts for the dynamic component associated with the local VGD and future SLR projections and therefore it enables decision-makers in tailoring Best Management Practices (BMPs) to local topographical characteristics and identifying the most suitable adaptation measures to cope with future sea levels with a higher resolution spatial scale. The approaches here proposed can be easily exported and applied for the characterization of areas with similar geomorphological features and therefore potentially prone to the impacts of expected sea-level rise.

In conclusion, it is possible to state that the hazard and risk assessments proposed in this study satisfy the EC requirements for addressing the climate adaptation and risk-reduction challenges in coastal areas by improving the knowledge of policymakers and local administrators and raising their awareness about the potential impacts of climate change on the territory and, therefore, promoting the mainstream of coastal adaptation strategies in national policy and regulations.

**Table 10** R3 and R4 risk classes evaluation for each municipality located in the study areas, expressed both as square kilometers and percentage of the surface falling within the plain sector

| Plain | Municipality | Total Surface of the Municipality ($km^2$) | % in the investigated area | R3_2065 | | R3_2100 | | R4_2065 | | R4_2100 | |
|---|---|---|---|---|---|---|---|---|---|---|---|
| | | | | *$km^2$* | *%* | *$km^2$* | *%* | *$km^2$* | *%* | *$km^2$* | *%* |
| Volturno Plain | Castelvolturno | 74.0 | 98.5 | 15.6 | 21.0 | 11.7 | 15.9 | 20.8 | 28.1 | 37.0 | 50.1 |
| | Giugliano in Campania | 94.6 | 6.0 | 0.3 | 0.4 | 0.3 | 0.3 | 4.0 | 4.2 | 4.3 | 4.5 |
| | Villa Literno | 61.8 | 55.1 | 2.9 | 4.6 | 2.5 | 4.1 | 17.1 | 27.7 | 20.0 | 32.3 |
| | Cancello ed Arnone | 49.3 | 73.4 | 1.1 | 2.3 | 2.9 | 6.0 | 0.8 | 0.8 | 2.6 | 5.3 |
| | Grazzanise | 47.1 | 1.4 | – | – | – | – | – | – | – | – |
| | Mondragone | 55.7 | 47.0 | 3.5 | 6.2 | 3.1 | 5.6 | 6.2 | 11.1 | 9.8 | 17.5 |
| | Carinola | 59.2 | 5.0 | – | – | – | – | – | – | – | – |
| | Falciano del Massico | 46.7 | 6.0 | – | – | 0.1 | 0.3 | – | – | – | – |
| Sarno Plain | Castellammare di Stabia | 17.8 | 10.3 | 0.1 | 0.8 | 0.4 | 1.9 | 0.1 | 0.4 | 0.2 | 1.1 |
| | Pompei | 12.4 | 8.4 | – | – | – | – | 0.1 | 0.4 | – | – |
| | Torre Annunziata | 7.5 | 1.7 | 0.1 | 1.1 | 0.2 | 2.2 | – | – | 0.1 | 1.7 |
| Sele Plain | Agropoli | 32.8 | 0.9 | – | – | – | – | – | – | – | – |
| | Capaccio | 113.0 | 20.0 | 0.2 | 0.2 | 0.8 | 0.7 | 0.1 | 0.1 | 0.2 | 0.2 |
| | Eboli | 137.6 | 16.2 | 2.8 | 2.1 | 3.8 | 2.7 | 2.5 | 1.8 | 5.5 | 4.0 |
| | Battipaglia | 56.9 | 9.2 | 0.9 | 1.6 | 1.4 | 2.4 | 0.0 | 0.1 | 0.1 | 0.2 |
| | Pontecagnano Faiano | 37.2 | 15.5 | 0.1 | 0.2 | 0.7 | 1.7 | 0.1 | 0.2 | 0.1 | 0.3 |
| | Salerno | 59.9 | 6.2 | 0.1 | 0.1 | 0.1 | 0.2 | – | 0.1 | 0.1 | 0.2 |
| Alento Plain | Ascea | 37.5 | 10.1 | 0.1 | 0.1 | 0.1 | 0.1 | – | – | 0.1 | 0.2 |
| | Casalvelino | 31.7 | 8.4 | 0.1 | 0.3 | 0.1 | 0.3 | – | 0.1 | 0.1 | 0.3 |
| | Castelnuovo Cilento | 18.1 | 1.6 | – | 0.1 | – | – | – | – | – | 0.1 |

**Authors' contributions** Conceptualization: Pietro P.C. Aucelli; Gianluigi Di Paola, Angela Rizzo; Methodology: Gianluigi Di Paola, Angela Rizzo, Fabio Matano, Pietro P.C. Aucelli; Formal analysis and investigation: Gianluigi Di Paola, Angela Rizzo, Giuseppe Corrado, Fabio Matano; Writing—original draft preparation: Angela Rizzo, Gianluigi Di Paola; Writing—review and editing: Angela Rizzo, Gianluigi Di Paola, Guido Benassai, Giuseppe Corrado, Fabio Matano, Pietro P.C. Aucelli; Funding acquisition: Pietro P.C. Aucelli; Supervision: Pietro P.C. Aucelli. All authors have read and agreed to the final version of the manuscript.

**Funding** Open access funding provided by Università degli Studi di Bari Aldo Moro within the CRUI-CARE Agreement. This study was financially supported by FFABR (MIUR – Ministry of Education, Universities and Research) and by a research fund granted to P.P.C. Aucelli by the University of Naples "Parthenope".

**Availability of data and material** LIDAR data have been provided by the Italian Ministry of the Environment. The datasets generated during and/or analyzed during the current study are available from the corresponding author on request.

**Code availability** Not applicable.

## Declarations

**Conflicts of interest** The authors declare no conflict of interest.

**Open Access** This article is licensed under a Creative Commons Attribution 4.0 International License, which permits use, sharing, adaptation, distribution and reproduction in any medium or format, as long as you give appropriate credit to the original author(s) and the source, provide a link to the Creative Commons licence, and indicate if changes were made. The images or other third party material in this article are included in the article's Creative Commons licence, unless indicated otherwise in a credit line to the material. If material is not included in the article's Creative Commons licence and your intended use is not permitted by statutory regulation or exceeds the permitted use, you will need to obtain permission directly from the copyright holder. To view a copy of this licence, visit http://creativecommons.org/licenses/by/4.0/.

## References

Aiello G, Amato V, Aucelli PPC, Barra D, Corrado G, Di Leo P, Di Lorenzo H, Jicha B, Pappone G, Parisi R, Petrosino P, Elda Russo E, Schiattarella M (2021) Multiproxy study of cores from the Garigliano plain: an insight into the Late Quaternary coastal evolution of Central-Southern Italy. Palaeogeogr Palaeoclimatol Palaeoecol 567:110298

Alberico I, Amato V, Aucelli PPC, D'Argenio B, Di Paola G, Pappone G (2012a) Historical shoreline evolution and recent shoreline trends of Sele Plain coastline (southern Italy). The 1870–2009 time window. J Coastal Res 28:1638–1647. https://doi.org/10.2112/JCOASTRES-D-10-00197

Alberico I, Amato V, Aucelli PPC, Di Paola G, Pappone G, Rosskopf CM (2012b) Historical and recent changes of the Sele River coastal plain (Southern Italy): natural variations and human pressures. Rend Fis Acc Lincei 23(1):3–12

Albore-Livadie C, Barra D, Bonaduce G, Brancaccio L, Cinque A, Ortolani F, Pagliuca S, Russo F (1990) Evoluzione geomorfologica, neotettonica e vulcanica della piana costiera del fiume Sarno (Campania) in relazione agli insediamenti anteriori all'eruzione del 79 d.C. In: Albore Livadie C, Widemann F (eds) Volcanologie et Archeologie. PACT, Consiglio d'Europa, vol 25, pp 237–256

Alexander D (2005) Towards the development of a standard in emergency planning, Disaster Prev. Manag 14:158–175. https://doi.org/10.1108/09653560510595164

alfresco/webdav/Siti/sit-regione-campania/CTR/CTR%20Edizione%20 2004–2005?rootFO=/

Amato V, Aucelli PPC, D'Argenio B, Da Prato S, Ferraro L, Pappone G, Petrosino P, Romano P, Rosskopf CM, Russo Ermolli E (2012) Holocene environmental evolution of the costal sector in front of the Poseidonia-Paestum archaeological area (Sele plain, Southern Italy). Rendiconti Lincei 23:45–59

Amato V, Aucelli PPC, Corrado G, Di Paola G, Matano F, Pappone G, Schiattarella M (2020) Comparing geological and Persistent Scatterer Interferometry data of the Sele River coastal plain, southern Italy: Implications for recent subsidence trends. Geomorphology 351:106953

Amorosi A, Pacifico A, Rossi A, Ruberti D (2012) Late Quaternary incision and deposition in an active volcanic setting: The Volturno valley fill, southern Italy. Sed Geol 282:307–320

Antonioli F, Anzidei M, Amorosi A, Lo Presti V, Mastronuzzi G, Deiana G, De Falco G, Fontana A, Fontolan G, Lisco S, Marsico A, Moretti M, Orrù PE, Sannino GM, Serpelloni E, Vecchio A (2017) Sea-level rise and potential drowning of the Italian coastal plains: Flooding risk scenarios for 2100. Quatern Sci Rev 158:29–43. https://doi.org/10.1016/j.quascirev.2016.12.021

Antonioli F, Defalco G, Moretti L, Anzidei M, Bonaldo D, Carniel S, Leoni G, Furlani S, Presti V, Mastronuzzi G, Petitta M, Vecchio A, Sannino G, Schicchitano G (2019) Relative sea level rise and potential flooding risk for 2100 on 15 coastal plains of the Mediterranean Sea. Geophys Res Abstr 21:5274

Antonioli F, Silenzi S (2007) Variazioni relative del livello del mare e vulnerabilità delle pianure costiere italiane. Quaderno della Società Geologica Italiana 2.

Anzidei M, Scicchitano G, Scardino G, Bignami C, Tolomei C, Vecchio A, Mastronuzzi G (2021) Relative Sea-Level Rise Scenario for 2100 along the Coast of South Eastern Sicily (Italy) by InSAR Data, Satellite Images and High-Resolution Topography. Remote Sens 13(6):1108

Armaroli C, Duo E (2017) Validation of the coastal storm risk assessment framework along the Emilia-Romagna coast. Coast Eng. https://doi.org/10.1016/j.coastaleng.2017.08.014

Ascione A, Aucelli PPC, Cinque A, Di Paola G, Mattei G, Ruello M, Russo EE, Santangelo N, Valente E (2020) Geomorphology of Naples and the Campi Flegrei: human and natural landscapes in a restless land. J Maps. https://doi.org/10.1080/17445647.2020.1768448

Aucelli PPC, Cinque A, Mattei G, Pappone G (2017a) Late Holocene landscape evolution of the Gulf of Naples (Italy) inferred from geoarchaeological data. J Maps 13(2):300–310

Aucelli PPC, Di Paola G, Incontri P, Rizzo A, Vilardo G, Benassai G, Buonocore B, Pappone G (2017b) Coastal inundation risk assessment due to subsidence and sea level rise in a Mediterranean alluvial plain (Volturno coastal plain-southern Italy). Estuar Coast Shelf Sci 198:597–609. https://doi.org/10.1016/j.ecss.2016.06.017

Aucelli PPC, Di Paola G, Rizzo A, Rosskopf CM (2018) Present day and future scenarios of coastal erosion and flooding processes along the Italian Adriatic coast: the case of Molise region. Environmental Earth Sciences 77:371. https://doi.org/10.1007/s12665-018-7535-y

Baldi P, Casula G, Cenni N, Loddo F, Pesci A (2009) GPS-based monitoring of land subsidence in the Po Plain (Northern Italy). Earth

Planet Lett 288:204212. https://doi.org/10.1016/j.epsl.2009.09.023

Ballesteros C, Jiménez JA, Viavattene C (2018) A multi-component flood risk assessment in the Maresme coast (NW Mediterranean). Nat Hazards 90(1):265–292

Barra D, Bonaduce G, Brancaccio L, Cinque A, Ortolani F, Pagliuca S, Russo F (1989) Holocene geological evolution of Sarno river coastal plain (Campania). Memorie Della Società Geologica Italiana 42:255–267

Barra D, Calderoni G, Cinque A, De Vita P, Rosskopf C, Russo Ermolli E (1998) New data on the evolution of the Sele river coastal plain (Southern Italy) during the Holocene. Il Quaternario 11(2):287–299

Barra D, Calderoni G, Cipriani M, La De, Geniere', J., Fiorillo, L., Greco, G., Mariotti Lippi, M., Mori Secci, M., Pescatore, T., Russo, B., Senatore, M.R., Tocco Sciarelli, G., Thorez, J. (1999) Depositional history and paleogeographic reconstruction of Sele coastal plain during Magna Grecia settlement of Hera Argiva (southern Italy). Geol Romana 35:151–166

Bates P, De Roo AP (2000) A simple raster-based model for flood inundation simulation. J Hydrol 236:54–77. https://doi.org/10.1016/S0022-1694(00)00278-X

Benassai G, Di Paola G, Aucelli P (2015) Coastal risk assessment of a micro-tidal littoral plain in response to sea level rise, Ocean Coast. Manage 104:22–35. https://doi.org/10.1016/j.ocecoaman.2014.11.015

Brambati A, Carbognin L, Quaia T, Teatini P, Tosi L (2003) The Lagoon of Venice: geological setting, evolution and land subsidence. Episodes 26:264–268

Brancaccio L, Cinque A, D'angelo, G., Russo, F., Santangelo, N. & Sgrosso, L., (1987) Evoluzione tettonica e geomorfologica della Piana del Sele (Campania, Appennino meridionale). Geogr Fis Dinam Quat 10:47–55

Brancaccio L, Cinque A, Romano P, Rosskopf C, Russo F, Santangelo N, Santo A (1991) Geomorphology and neotectonic evolution of a sector of the Tyrrhenian flank of the Southern Apennines (Region of Naples, Italy). Zeit. Geomorph. Suppl 82:47–58

Brancaccio L, Cinque A, Romano P, Rosskopf C, Russo F, Santangelo N (1995) L'evoluzione delle pianure costiere della Campania: geomorfologia e neotettonica. Memorie Della Società Geografica Italiana 53:313–336

Brancaccio, L., Cinque, A., Russo, F., Santangelo, N., Alessio, M., Allegri, L., Improta, S., Belluomoni, G., Branca, M., Delitala, L., 1988. Nuovi dati cronologici sui depositi marini e continentali della piana del F. Sele e della costa settentrionale del Cilento, Atti 74° Congr. Soc. Geol. It., vol. A, Sorrento, pp. 55–62.

Buonocore B, Cotroneo Y, Capozzi V, Aulicino G, Zambardino G, Budillon G (2020) Sea-Level Variability in the Gulf of Naples and the "Acqua Alta" Episodes in Ischia from Tide-Gauge Observations in the Period 2002–2019. Water 12(9):2466

Regione Campania (2009) Progetto TELLUS web page. http://www.difesa.suolo.regione.campania.it/content/category/4/64/92/. Accessed 10 June 2019.

Regione Campania, 2009. Settore Difesa del Suolo. Progetto TELLUS web page. http://www.difesa.suolo.regione.campania.it/content/category/4/64/92/. Accessed 3 September 2017

Casciello E, Cesarano M, Pappone G (2006) Extensional detachment faulting on the Tyrrhenian margin of the southern Apennines contractional belt (Italy). J Geol Soc 163:617–629

Provincia di Caserta (2009) Piano Territoriale di Coordinamento provinciale - Territorio insediato: Infrastrutture trasporto e produzione dell'energia. (B5.6.1 e B5.6.2) http://www.provincia.caserta.it/ptc/B%20Elaborati%20grafici%20del%20quadro%20conoscitivo/B5%20Territorio%20insediato/. Accessed 13 April 2019.

Catalao J, Raju D, Nico G (2020) InSAR maps of land subsidence and sea level scenarios to quantify the flood inundation risk in coastal cities: The case of Singapore. Remote Sensing 12(2):296

Cenni N, Viti M, Baldi P, Mantovani E, Bacchetti M, Vannucchi A (2013) Present vertical movements in Central and Northern Italy from GPS data: possible role of natural and anthropogenic causes. J Geodyn 2013(71):74–85

Chen X, Zhang X, Church JA, Watson CS, King MA, Monselesan D, Legresy B, Harig C (2017) The increasing rate of global mean sea-level rise during 1993–2014. Nat Clim Chang 7(7):492–495. https://doi.org/10.1038/nclimate3325

Cinque A (1991) The versilian transgression in the Sarno River plain (Campania). Geogr Fis Dinam Quat 14:63–71

Cinque A, Irollo G (2004) Il "Vulcano di Pompei": nuovi dati geomorfologici e stratigrafici. Il Quaternario 17(1):101–116

Cinque A, Rosskopf C, Barra D, Campajola L, Paolillo G, Romano M (1995) Nuovi dati stratigrafici e cronologici sull'evoluzione recente della piana del fiume Alento (Cilento, Campania). Il Quaternario, Italian Journal of Quaternary Sciences 8(2):323–338

Città Metropolitana di Napoli, 2015. Piano Territoriale di Coordinamento - Sorgenti di Rischio Ambientali. https://www.cittametropolitana.na.it/documents/10181/1822919/A05-0%20-%20Sorgenti%20di%20rischio%20ambientale.pdf/3ea29936-97cb-4cf2-b575-093577ef40cd (accessed on 13 April 2019)

Copernicus Climate Change Service (C3S), 2020. Water level change indicators for the European coast from 1977 to 2100 derived from climate projections. https://doi.org/10.24381/cds.b6473cc1

Corrado G, Amodio S, Aucelli PPC, Incontri P, Pappone G, Schiattarella M (2018) Late quaternary geology and morphoevolution of the Volturno coastal plain, southern Italy. Alpine and Mediterranean Quaternary 31:23–26

Corrado G, Amodio S, Aucelli PPC, Pappone G, Schiattarella M (2020) The Subsurface Geology and Landscape Evolution of the Volturno Coastal Plain, Italy: Interplay between Tectonics and Sea-Level Changes during the Quaternary. Water 12:3386

Costantini, M.; Falco, S., Malvarosa, F., Minati, F., Trillo, F., (2009). Method of Persistent Scatterer Pairs (PSP) and high resolution SAR interferometry. In Proceedings of the 2009 IEEE International Geoscience and Remote Sensing Symposium (IGARSS), Cape Town, South Africa, 12–17 July 2009; Volume 3, pp. 904–907.

CTR, 2004. Carta Tecnica Regionale della Regione Campania https://sit2.regione.campania.it/

Dangendorf S, Hay C, Calafat FM, Marcos M, Piecuch CG, Berk K, Jensen J (2019) Persistent acceleration in global sea-level rise since the 1960s. Nat Clim Chang 9(9):705–710

De Pippo T, Donadio C, Pennetta M, Petrosino C, Terlizzi F, Valente A (2008) Coastal hazard assessment and mapping in Northern Campania. Italy Geomorphology 97(451–466):2008

Di Paola G, Aucelli PP, Benassai G, Rodríguez G (2014) Coastal vulnerability to wave storms of Sele littoral plain (southern Italy). Nat Hazards 71:1795–1819. https://doi.org/10.1007/s11069-013-0980-8

Di Paola G, Alberico I, Aucelli PPC, Matano F, Rizzo A, Vilardo G (2018) Coastal subsidence detected by Synthetic Aperture Radar interferometry and its effects coupled with future sea-level rise: the case of the Sele Plain (Southern Italy). Journal of Flood Risk Management 11(2):191–206. https://doi.org/10.1111/jfr3.12308

Dieng HB, Cazenave A, Meyssignac B, Ablain M (2017) New estimate of the current rate of sea level rise from a sea level budget approach. Geophys Res Lett 44(8):3744–3751

Donadio C, Vigliotti M, Valente R, Stanislao CI, R., Ruberti D., (2018) Anthropic vs. natural shoreline changes along the northern Campania coast. Italy J Coast Conserv 22:939–955. https://doi.org/10.1007/s11852-017-0563-z

Dottori F, Szewczyk W, Ciscar JC, Zhao F, Alfieri L, Hirabayashi Y, Bianchi A, Mongelli I, Frieler K, Betts RA, Feyen L (2018) Increased human and economic losses from river flooding with anthropogenic warming. Nat Clim Chang 8(9):781–786. https://doi.org/10.1038/s41558-018-0257-z

EC, 2007. Directive 2007/60/EC of the European parliament and of the council, of 23 October 2007 on the assessment and management of flood risks, https://eur-lex.europa.eu/legal-content/EN/TXT/PDF/?uri=CELEX:32007L0060&from=EN (accessed on 7 Jun 2019).

EC, 2013. Communication from the commission to the European parliament, the council, the European economic and social committee and the committee of the regions. An EU Strategy on adaptation to climate change https://eur-lex.europa.eu/legal-content/EN/TXT/PDF/?uri=CELEX:52013DC0216&from=EN (accessed on 7 Jun 2019).

EEA, 2019. The Adaptation Support Tool – Getting started. How is the European climate changing? https://climate-adapt.eea.europa.eu/knowledge/tools/adaptation-support-tool/european-climate (accessed on 20 November 2019).

EPRS, 2015. Not-Ordinary Plan of Environmental Remote Sensing Web Page. National Geoportal (NG) of the Italian Ministry of Environment and of Protection of Territory and Sea. http://www.pcn.minambiente.it/GN/en/projects/not-ordinary-plan-of-remote-sensing (accessed on 20 November 2019).

EUROSION, 2004. Living with coastal erosion in Europe: sediment and space for sustainability. Reports on-line. http://www.eurosion.org (accessed on 20 March 2019).

Ferreira O, Viavattene C, Jimenez J, Bolle A, das Neves L., Plomaritis T., McCall R., Van Dongeren, (2017) Storm-induced risk assessment: evaluation of two tools at the regional and hotspot scale. Coast Eng. https://doi.org/10.1016/j.coastaleng.2017.10.005

Ferretti A, Prati C, Rocca F (2001) Permanent scatterers in SAR interferometry. IEEE Trans Geosci Remote Sens 39(1):8–20

Ferretti A, Savio G, Barzaghi R, Borghi A, Musazzi S, Novali F, Prati C, Rocca F (2007) Sub-millimeter accuracy of InSAR time series: experimental validation. IEEE Transactions on Geoscience Remote Sensing 45(5):1142–1153. https://doi.org/10.1109/TGRS.2007.894440

Frasca, M., 2018. Castelvolturno (Caserta), Consortile sott'acqua e famiglie costrette in casa a Destra Volturno. https://cronachedi.it/2018/03/22/castelvolturno-caserta-consortile-sottacqua-famiglie-costrette-casa-destra-volturno/ (accessed on 23 November 2019).

Giaccio B, Hajdas I, Isaia R, Deino A, Nomade S (2017) High-precision $^{14}C$ and $^{40}Ar/^{39}Ar$ dating of the Campanian Ignimbrite (Y-5) reconciles the time-scales of climatic-cultural processes at 40 ka. Sci Rep 7:45940

Houghton LG, Meira Filho LG, Callander BA (1996) Climate change 1995: the science of climate change. Cambridge University Press, Cambridge

IPCC (2014) Fifth assessment report—climate change. Impacts, adaptation and vulnerability: regional aspects. Cambridge University Press, Cambridge

IPCC (2019) Climate Change and Land: an IPCC special report on climate change, desertification, land degradation, sustainable land management, food security, and greenhouse gas fluxes in terrestrial ecosystems, https://www.ipcc.ch/srccl/. Accessed on 30 November 2019).

Ippolito F, Ortolani F, Russo M (1973) Struttura marginale tirrenica dell'Appennino campano: reinterpretazione di dati di antiche ricerche di idrocarburi. Mem Soc Geol It 12:227–251

ISTAT (2019) http://ottomilacensus.istat.it/. Accessed 7 Jun 2019.

Kruse S, Abeling T, Deeming H, Fordham M, Forrester J, Jülich S, Karanci AN, Kuhlicke C, Pelling M, Pedoth L, Schneiderbauer S (2017) Conceptualizing community resilience to natural hazards – the emBRACE framework. Nat Hazards Earth Syst Sci 17:2321–2333. https://doi.org/10.5194/nhess-17-2321-2017

Lambeck K, Antonioli F, Anzidei M, Ferranti L, Leoni G, Scicchitano G, Silenzi S (2011) Sea level change along the Italian coast during the Holocene and projections for the future. Quatern Int 232:250–257

Le Cozannet G, Idier D, de Michele M, Legendre Y, Moisan M, Pedreros R, de la Torre Y (2021) Timescales of emergence of chronic flooding in the major economic center of Guadeloupe. Nat Hazard 21(2):703–722

Mastrocicco M, Busico G, Colombani N, Vigliotti M, Ruberti D (2019) Modelling actual and future seawater intrusion in the variconi coastal wetland (italy) due to climate and landscape changes. Water 11:1502. https://doi.org/10.3390/w11071502

Matano F (2019) Analysis and classification of natural and human-induced ground deformations at regional scale (campania, italy) detected by satellite synthetic-aperture radar interferometry archive datasets. Remote Sens 11(23):2822. https://doi.org/10.3390/rs11232822

Matano F, Sacchi M, Vigliotti M, Ruberti D (2018) Subsidence trends of volturno river coastal plain (Northern Campania, Southern Italy) inferred by SAR interferometry data. Geosciences 8:8. https://doi.org/10.3390/geosciences8010008

Mattei G, Rizzo A, Anfuso G, Aucelli PPC, Gracia FJ (2019) A tool for evaluating the archaeological heritage vulnerability to coastal processes: The case study of Naples Gulf (southern Italy). Ocean Coastal Manage 179:104876

Mattei G, Rizzo A, Anfuso G, Aucelli PPC, Gracia FJ (2020) Enhancing the protection of archaeological sites as an integrated coastal management strategy: The case of the Posillipo Hill (Naples, Italy). Rendiconti Lincei Scienze Fisiche e Naturali 2020:1–14

MATTM (2017) Ministry of the environment and protection of land and sea. http://www.pcn.minambiente.it/mattm/progetto-coste. Accessed 5 June 2017.

Moccia M (2018) Le mareggiate mettono in ginocchio Castel Volturno, enormi danni ai lidi e disagi per i cittadini. https://casertaweb.com/notizie/le-mareggiate-mettono-ginocchio-castel-volturno-enormi-danni-ai-lidi-disagi-cittadini/. Accessed 23 Nov 2019.

Nerem RS, Beckley BD, Fasullo JT, Hamlington BD, Masters D, Mitchum GT (2018) Climate-change–driven accelerated sea-level rise detected in the altimeter era. Proc Natl Acad Sci 115(9):2022–2025

Nicholls RJ (2010) Impacts of and responses to sea-level rise. In: Church JA, Woodworth PL, Aarup T, Wilson WS (eds) Understanding sea-level rise and variability. Wiley-Blackwell, Oxford

Pappone G, Alberico I, Amato V, Aucelli PPC, Di Paola G (2011) Recent evolution and the present-day conditions of the Campanian Coastal plains (South Italy): the case history of the Sele River Coastal plain. WIT Trans Ecol Environ 149:15–27. https://doi.org/10.2495/CP110021

Pappone G, Aucelli PPC, Alberico I, Amato V, Antonioli F, Cesarano M, Di Paola G, Pelosi N (2012) Relative sea-level rise and marine erosion and inundation in the Sele River coastal plain (Southern Italy): scenarios for the next century. Rendiconti Lincei 23:121–129. https://doi.org/10.1007/s12210-012-0166-4

Patacca E, Sartori R, Scandone P (1990) Tyrrhenian basin and Apenninic arcs: kinematic relations since Late Tortonian times. Memorie Società Geologica Italiana 45:425451

Pennetta M, Stanislao C, D'Ambrosio V, Marchese F, Minopoli C, Trocciola A, Valente R, Donadio C (2016) Geomorphological features of the archaeologicalmarine area of Sinuessa in Campania, southern Italy. Quatern Int 425:198–213. https://doi.org/10.1016/j.quaint.2016.04.019

Perini L, Calabrese L, Salerno G, Ciavola P, Armaroli C (2016) Evaluation of coastal vulnerability to flooding: comparison of two

different methodologies adopted by the Emilia-Romagna region (Italy). Nat Hazards Earth Syst Sci 16:181–194
Piano Stralcio Erosione Costiera, 2012. Relazione Tecnica. https://www.distrettoappenninomeridionale.it/images/_PAI/LGV/Relazione%20tecnica%20PSEC.pdf. Accessed 10 June 2019
Poulter B, Halpin PN (2008) Raster modelling of coastal flooding from sea-level rise. Int J Geogr Inf Sci 22:167–182. https://doi.org/10.1080/13658810701371858
Provincia di Caserta, 2012. Piano Territoriale di Coordinamento della Provincia di Salerno - Le caratteristiche antropiche del territorio: Reti ed Impianti per l'energia. http://geoportale.provincia.salerno.it/sites/default/files/ptcp/Serie%201/1_7_6.pdf. Accessed 13 April 2019.
La Repubblica, 2019. Maltempo, Campania: allerta meteo Arancione fino alle 23.59 di domani. https://napoli.repubblica.it/cronaca/2019/12/21/news/maltempo_campania-244017655/ (accessed on 28 December 2019).
Rizzo A, Vandelli V, Buhagiar G, Micallef AS, Soldati M (2020) Coastal vulnerability assessment along the North-Eastern sector of Gozo Island (Malta, Mediterranean Sea). Water 12(5):1405
Romano P, Santo A, Voltaggio M (1994) L'evoluzione geomorfologica della pianura del Fiume Volturno (Campania) durante il tardo Quaternario (Pleistocene medio-superiore—Olocene). Il Quaternario 1994:41–56
Rovere A, Furlani S, Benjamin J, Fontana A, Antonioli F (2012) MEDFLOOD project: MEDiterranean sea-level change and projection for future FLOODing. Alp Mediterr Quat 25(2):36
Ruberti D, Vigliotti M (2017) Land use and landscape pattern changes driven by land reclamation in a coastal area: the case of Volturno delta plain, Campania Region, southern Italy. Environ Earth Sci 76:694. https://doi.org/10.1007/s12665-017-7022-x
Ruberti D, Mandolini A, Matano F, Picarelli L, Sacchi M, Vigliotti M (2017) Holocene stratigraphic architecture and current land subsidence of the Volturno coastal plain (northern Campania, southern Italy). J Medit Earth Sci 9:193–196. https://doi.org/10.3304/JMES.2017.004
Ruberti D, Sacchi M, Pepe F, Vigliotti M (2018a) LGM Incised Valley in a volcanic setting. The Northern Campania Plain (Southern Italy). Alpine and Mediterranean Quaternary 31:35–38
Ruberti D, Vigliotti M, Di Mauro A, Chieffi R, Di Natale M (2018b) Human influence over 150 years of coastal evolution in the Volturno delta system (southern Italy). J Coast Conserv 22:897–917. https://doi.org/10.1007/s11852-017-0557-x
Russo F, Belluomini G (1992) Affioramenti di depositi marini tirreniani sulla piana in destra del Fiume Sele (Campania). Boll Soc Geol 111:25–31
Sacchi M, Molisso F, Pacifico A, Vigliotti M, Sabbarese C, Ruberti D (2014) Late-Holocene to recent evolution of Lake Patria, South Italy: An example of a coastal lagoon within a Mediterranean delta system. Global Planet Change 117:9–27
Santo A, Santangelo N, De Falco M, Forte G, Valente E (2019) Sinkholes in alluvial plain: the prehistoric case study of "Fossa San Vito" (Sarno-Southern Italy). Geomorphology 345:106838
Schaeffer M, Hare W, Rahmstorf S, Vermeer M (2012) Long-term sea-level rise implied by 1.5 °C and 2 °C warming levels. Nat Clim Chang 2(12):867–870. https://doi.org/10.1038/nclimate1584
Copernicus Climate Change Service (C3S), 2018. Sea level. https://climate.copernicus.eu/sea-level.
Shirzaei M, Bürgmann R (2018a) Global climate change and local land subsidence exacerbate inundation risk to the San Francisco Bay Area. Sci Adv 4(3):eaap9234
Shirzaei M, Bürgmann R (2018b) Global climate change and local land subsidence exacerbate inundation risk to the San Francisco Bay Area. Sci Adv 4(3):9234
Siti/sit-regione-campania/CTR (accessed on 5 April 2019).
Spano, D., Mereu, V., Bacciu, V., Marras, S., Trabucco, A., Adinolf, M., Zavatarelli, M. (2020). Analisi del rischio. I cambiamenti climatici in Italia. CMCC
Teatini P, Tosi L, Strozzi T, Carbognin L, Cecconi G, Rosselli R, Libardo S (2012) Resolving land subsidence within the Venice Lagoon by persistent scatterer SAR interferometry. Phys Chem Earth 40–41:72–79. https://doi.org/10.1016/j.pce.2010.01.002
Valente E, Ascione A, Santangelo N, Santo A (2019) Late Quaternary geomorphological evolution and evidence of post-campania ignimbrite (40 ka) fault activity in the inner sector of the Sarno Plain (Southern Apennines, Italy). Alpine and Mediterranean Quaternary 32(2):185–197
Viavattene, C., Jimenez, J., Owen D., Priest, S.J., Parker, D.J., Micou, P., Ly S, 2015. Coastal risk assessment framework: guidance document. Deliv No. D23155. http://eprints.mdx.ac.uk/id/eprint/1853. Accessed on 19 January 2017.
Vilardo, G., Ventura, G., Terranova, C., Matano, F., Nardo, S., 2009. Ground deformation due to tectonic, hydrothermal, gravity, hydrogeological, and anthropic processes in the Campania region (southern Italy) from permanent scatterers synthetic aperture radar interferometry.
Vousdoukas MI, L., Mentaschi, E., Voukouvalas, A. Bianchi, F. Dottori, L. Feyen, (2018) Climatic and socioeconomic controls of future coastal flood risk in Europe. Nature Clim Change 8:776–780. https://doi.org/10.1038/s41558-018-0260-4
Vousdoukas MI, Mentaschi L, Hinkel J, Ward PJ, Mongelli I, Ciscar JC, Feyen L (2020) Economic motivation for raising coastal flood defenses in Europe. Nat Commun 11(1):1–11
Warrick RA, Oerlemans J, Woodworth PL, Meier MF, le Provost C (1996) Changes in sea level. In: Houghton JT, Meira Filho LG, Callander BA (eds) Climate Change 1995: the Science of Climate Change. Cambridge University Press, Cambridge, p 359e405
WMO (2017) Guidelines on the Calculation of Climate Normals.
World Meteorological Organization (WMO) (2019) The Global Climate in 2015–2019. https://library.wmo.int/index.php?lvl=notice_display&id=21522#.YCZmRGhKjIW.
Wright, L.D., Syvitski, J.P.M., Nichols, C.R., 2019. Sea Level Rise: Recent Trends and Future Projections. In: Wright L., Nichols C. (eds) Tomorrow's Coasts: Complex and Impermanent. Coastal Research Library, vol 27, https://doi.org/10.1007/978-3-319-75453-6_3.
Yi S, Heki K, Qian A (2017) Acceleration in the global mean sea level rise: 2005–2015. Geophys Res Lett 44(11):905–913

**Publisher's Note** Springer Nature remains neutral with regard to jurisdictional claims in published maps and institutional affiliations.